Materials Science & Engineering C 110 (2020) 110727

Contents lists available at ScienceDirect

Materials Science & Engineering C

journal homepage: www.elsevier.com/locate/msec

Enhanced antibacterial activity of calcium silicate-based hybrid cements for bone repair

Ming-Cheng Lin[a], Chun-Cheng Chen[b,c], I-Ting Wu[d,*], Shinn-Jyh Ding[a,b,**]

[a] Institute of Oral Science, Chung Shan Medical University, Taichung City 402, Taiwan
[b] Department of Stomatology, Chung Shan Medical University Hospital, Taichung City 402, Taiwan
[c] School of Dentistry, Chung Shan Medical University, Taichung City 402, Taiwan
[d] Department of Periodontology, China Medical University Hospital, Taichung City 404, Taiwan

ARTICLE INFO

Keywords:
Calcium silicate
Bone cement
Chitosan
Anti-washout
Antibacterial activity

ABSTRACT

Calcium silicate cement has attracted much attention for bone defect repair and regeneration due to its osteogenic properties. Biomaterial-associated infections and washout have become a common clinical problem. In order to enhance the antibacterial and washout performance of calcium silicate cement to meet clinical needs, different types of chitosan, including chitosan polysaccharide (CTS), quaternary ammonium chitosan (QTS), and chitosan oligosaccharide (COS), as a liquid phase were added to the calcium silicate powder. The physicochemical properties, in vitro bioactivity, antibacterial efficacy, and osteogenic effects (MG63 cells) of the cement were evaluated. Antibacterial activity was conducted with Gram-negative *Escherichia coli* (*E. coli*) and a Gram-positive *Staphylococcus aureus* (*S. aureus*) bacteria. The amount of intracellular reactive oxygen species (ROS) produced in the bacteria cultured with the chitosan solution was also detected. The experimental results showed that the chitosan additive did not affect the crystalline phase of calcium silicate cement, but increased the setting time and strength of the cement in a concentration-dependent manner. Within the scope of this study, CTS and QTS solutions with a concentration of not < 1 wt% improved the washout resistance of the control cement, while the COS solutions failed to strengthen the cement. When soaked in simulated body fluid (SBF) for 1 day, all cement samples formed apatite spherules. As the soaking time increased, the diametral tensile strength of all cements decreased and the porosity increased. The assays of MG63 cell function showed lower osteogenic activity of osteoblastic cells grown on the surfaces of the chitosan-incorporated cements in comparison with the control cement without chitosan. At the same 1% concentration, compared with QTS and COS cement, CTS cement had lower cell attachment, proliferation, differentiation, and mineralization. Conversely, the CTS cement resulted in the highest bacteriostasis ratio among the three hybrid cements against two bacteria. The ROS production followed the order of CTS > QTS > COS at the same 1% concentration. In conclusion, calcium silicate cement with 1% QTS may be a viable candidate for bone defect repair in view of anti-washout performance, setting time, antibacterial activity, and osteogenic activity shown in this study.

1. Introduction

The clinical need for bone defect repair and regeneration has motivated many efforts to develop innovative biomaterials [1–5], in addition to the use of autografts. With the increasing popularity of minimally invasive techniques, the development of injectable in situ setting systems has attracted a great deal of attention [1,3,5]. Calcium silicate (CaSi)-based materials can promote adhesion, growth, and differentiation of osteoblasts and have been used in many clinical applications [6,7]. On the other hand, even after treatment in infected bone defects, materials with high antibacterial activity help to reduce or limit the growth of any residual bacteria [8,9]. CaSi-based materials have also been shown to produce some degree of bacteriostatic action against various bacterial strains [4,10] because these materials can cause alkalization of the environment surrounding the materials. However, the antibacterial activity of CaSi is insufficient to effectively eliminate bacteria at the implanted bone defect. The ideal bone cement should promote the osteogenic activity of osteoblasts while inhibiting the growth of bacteria. The antibiotic-loaded bone cement is recognized as an adjunct for the treatment of established infections, but its role in

* Corresponding author.
** Correspondence to: S.-J. Ding, Institute of Oral Science, Chung Shan Medical University, Taichung 402, Taiwan.
E-mail addresses: tinyiting@gmail.com (I.-T. Wu), sjding@csmu.edu.tw (S.-J. Ding).

https://doi.org/10.1016/j.msec.2020.110727
Received 30 November 2019; Received in revised form 11 January 2020; Accepted 3 February 2020
Available online 04 February 2020
0928-4931/

preventing infection is still controversial because of issues regarding bacterial drug resistance, efficacy, and cost [2,5]. Therefore, it is necessary to develop a new type of CaSi cement without antibiotics to enhance the antibacterial effect.

Antibacterial materials are attractive in a variety of medical applications. The use of antimicrobial agents helps to address the challenges posed by drug-resistant bacterial infections. Among the antibacterial materials, the naturally occurring chitosan polysaccharide (CTS) is known for its bactericidal action against a broad spectrum of microorganisms [11–13]. Wu et al. have used hydroxypropyltrimethyl ammonium chloride chitosan (HACC) to improve the antibacterial ability of calcium phosphate cement (CPC) [14]. Interestingly, the HACC-containing CPC has no cytotoxic effects on mouse pluripotent C3H10T1/2 and murine L929 fibroblast cells. Recently, Youssef's group have reported that CaSi/chitosan-based composites exhibited good antibacterial activity against Gram positive, Gram negative bacteria and fungi [15,16]. Chitosan polysaccharides are obtained by the deacetylation of natural chitin and their structurally is similar to various glycosaminoglycans [12]. Linear amino-polysaccharide chitosan consisting of randomly distributed β-(1-4)-linked D-glucosamine (deacetylated unit) and *N*-acetyl-D-glucosamine (acetylated unit) always has very high molecular weight and viscosity [12,13,17]. Due to its numerous desirable properties, such as non-antigenicity, antioxidant, antibacterial activity, high hydrophilicity, and good film-forming properties, chitosan polysaccharides have become a natural choice for biomedical and edible packaging applications [18–21]. In addition, its positive charge can react with many negatively charged surfaces/polymers to form functionalized multilayer composites [22,23]. Lee et al. prepared a chitosan-alginate complex to enhance the washout-resistant ability of CPC [23]. On the other hand, chitosan polysaccharides may have better antibacterial ability in acidic environments due to better solubility [17]. However, their poor solubility above pH 6.5 limits the clinical applications [24]. Chitosan contains three distinct functional groups: a primary amino group and two hydroxyl groups (primary and secondary), which can be synthetically modified to obtain derivatives with improved biological properties [25]. Therefore, some water-soluble chitosan derivatives such as quaternary ammonium chitosan (QTS) and chitosan oligosaccharide (COS) have been synthesized [17,24,25]. Antibacterial activities of QTS has been shown to increase with increasing chain length of the alkyl substituent [26], which has more positive charge than CTS. In the case of COS, the anticancer and antibacterial bioactivity, low viscosity, and greater solubility of COS at neutral pH have attracted the interest of many researchers [19].

To greatly enhance the antibacterial activity of promising CaSi cement, non-antibiotic antibacterial ingredients can be added to the material. To this end, three different chitosan types (including CTS, QTS, and COS) were added as a liquid phase to the CaSi powder to form cement. An appropriate proportion of liquid would effectively promote the physicochemical and biological properties of CaSi hybrid cement, making it suitable for a wider range of clinical applications. Therefore, the purpose of this study was to optimize the performance of CaSi–chitosan hybrid cement by adjusting the amount and type of chitosan. The major assays used to characterize various cement samples included setting time, anti-washout property, in vitro bioactivity, antimicrobial efficacy, and in vitro osteogenic activity.

2. Materials and methods

2.1. Preparation of powder

Calcium silicate powder was prepared by using a sol-gel method as described elsewhere [27]. Reagent grade tetraethyl orthosilicate (TEOS, $Si(OC_2H_5)_4$; Sigma-Aldrich, St. Louis, MO, USA) and calcium nitrate (Ca $(NO_3)_2{\cdot}4H_2O$; Showa, Tokyo, Japan) were used as precursors for SiO_2 and CaO, respectively. Nitric acid and ethanol were used as the catalyst and solvent, respectively. Briefly, TEOS was hydrolyzed by sequential adding 2 M HNO_3 and absolute ethanol with 1 h of stirring, respectively. $Ca(NO_3)_2{\cdot}4H_2O$ was added to the TEOS solution in an equimolar ratio, and the mixture was further stirred for 1 h. The molar ratio of (HNO_3 + H_2O)-TEOS-ethanol was 10:1:10. The sol solution was sealed and aged at 60 °C for 1 day. After evaporating the solvent in an oven at 120 °C, the dried gel was heated in air to 800 °C for 2 h at a heating rate of 10 °C/min, and then cooled to room temperature in the furnace to produce a powder. The powders were then ball-milled in ethyl alcohol for 12 h using a Retsch S 100 centrifugal ball mill (Hann, Germany) and dried in an oven at 60 °C.

2.2. Preparation of liquid

Chitosan polysaccharide with 85% deacetylation derived from crab shells and water-soluble chitosan oligosaccharide with 90% deacetylation (molecular weight < 5 kDa) were purchased from Sigma-Aldrich and used without further purification. CTS solutions (0.1, 0.5, and 1 *w/v*%) were prepared in 2% acetic acid, while three different COS concentrations (1, 5, and 10 w/v%) were obtained by dissolving the powder in distilled water. For preparation of quaternary ammonium chitosan, CTS was dissolved in acetic acid and then desired amount of acetic anhydride (Echo Chemicals, Miaoli, Taiwan) was added. After stirring, NaOH was added to stop the reaction, and the mixture was dialyzed against water and freeze-dried. Thus, water-soluble *N*-acetylated chitosan was produced [28]. After that, on the basis of a modified method [29], glycidyltrimethylammonium chloride (GTMAC; Tokyo Chemical Industry Co., Ltd., Tokyo, Japan) was added dropwise to 2.5% water-soluble chitosan at a volume ratio of 4:1. The reaction was carried out for 8 h. GTMAC was used as a quarternizing agent because it has a quaternary ammonium group. After stirring, the product was placed in cold acetone and kept in a refrigerator for 24 h. The acetone was poured off and the remaining was dissolved in methanol for 1 h. The reaction mixture was precipitated in 4:1 acetone–ethanol solution, followed by filtration and drying at 60 °C to obtain QTS. Three concentrations of 0.5, 1, and 5 *w/v*% were prepared by dissolving the powder in distilled water.

2.3. Characterization of liquid

The chemical structures of CTS, QTS, and COS were examined by Fourier transform infrared spectroscopy (FTIR; Bruker Vertex 80v, Ettlingen, Germany) in transmittance mode, with a spectral resolution of 1 cm^{-1} at a wavenumber range of 400 to 4000 cm^{-1}. The powder was mixed with KBr and compressed into a pellet. Viscosity measurements were made on three types of 1% chitosan solutions using a Discovery HR-2 rheometer (TA Instruments, New Castle, USA) at room temperature using parallel plate geometry (25 mm diameter). The static rheological technique examined the relationship between the viscosity (η) of the chitosan solution and the shear rate. The samples were measured at shear rates from 0.1 to 500 s^{-1} with 10 data points per decade.

2.4. Cement preparation

Cement samples were prepared by manually mixing each powder with a liquid at a liquid-to-powder ratio of 0.5 mL/g. After mixing, the sample was placed into a cylindrical Teflon mold at a uniaxial pressure of 0.7 MPa for 1 min to form a sample having a size of 6 mm (diameter) × 3 mm (height) and stored in an incubator at 100% relative humidity and 37 °C for 1 day for hydration, unless otherwise stated (for example, anti-washout and setting time examination). The sample code "CT05" represented cement derived from 0.5% CTS, and the sample code "QT5" was cement after mixing powder with 5 wt% QTS, as listed in Table 1.

Table 1
Setting time, pH value, diametral tensile strength, and porosity of various bone cements prepared by different liquid compositions.

Sample code	Liquid	Concentration (wt%)	Setting time (min)	pH	Strength (MPa)	Porosity (%)
CS	H_2O		18 ± 2[a]	11.7 ± 0.1[a,b]	2.5 ± 0.4[a]	18 ± 1[a]
CT01	CTS	0.1	19 ± 1[a]	10.5 ± 0.1[c]	3.1 ± 0.2[a,b]	16 ± 2[a]
CT05		0.5	37 ± 2[b]	10.5 ± 0.1[c]	3.1 ± 0.2[a,b]	17 ± 2[a]
CT1		1	100 ± 1[c]	10.6 ± 0.1[c]	3.4 ± 0.4[b]	18 ± 1[a]
QT05	QTS	0.5	27 ± 1[d]	11.6 ± 0.1[b,d]	3.2 ± 0.2[b]	16 ± 2[a]
QT1		1	34 ± 1[e]	11.7 ± 0.1[a,b]	3.3 ± 0.2[b]	17 ± 2[a]
QT5		5	41 ± 1[f]	11.9 ± 0.1[a]	3.5 ± 0.3[b,c]	16 ± 1[a]
CO1	COS	1	20 ± 1[a]	11.4 ± 0.1[d,e]	2.7 ± 0.4[a]	16 ± 2[a]
CO5		5	30 ± 1[g]	11.2 ± 0.1[e]	2.9 ± 0.3[a,b]	17 ± 2[a]
CO10		10	41 ± 2[f]	11.1 ± 0.1[e]	3.1 ± 0.2[a,b]	18 ± 1[a]

Values are mean ± standard deviation. Mean values followed by the same superscript letter in a column were not significantly different ($p > 0.05$) according to Scheffe's post hoc multiple comparisons.

2.5. Anti-washout property

The anti-washout performance of cement samples was observed by visual inspection [30]. After mixing, the cement was molded in a cylindrical Teflon mold under a uniaxial pressure of 0.7 MPa for 1 min to form a sample size of 6 mm (diameter) × 6 mm (height). They were then removed from the mold and immediately placed into water at room temperature. If the cement did not disintegrate remarkably in water after 1 h, the sample was considered to have passed the washout resistance test.

2.6. Setting time and pH value

After mixing the powder with the liquid, the pH of each cement sample was immediately measured with a pH meter (model SP-701, SUNTEX, Taipei, Taiwan). Three parallel experiments were conducted with the data of every group. The setting time of cement was tested by using a 400-g Gillmore needle with a 1-mm diameter, according to ISO 9917-1 for water-based cements. The setting time was defined as the time during which the needle failed to produce an indentation of 1 mm depth in three separate areas of the cement at 100% relative humidity and 37 °C. The setting time of six samples was measured for each cement group.

2.7. Phase composition and morphology

The phase analysis of the cement surface was performed by an X-ray diffractometer (XRD; Bruker D8 SSS, Bruker Corporation, Karlsruhe, Germany) with Ni-filtered CuKα radiation operating at 40 kV and 100 mA with a scanning speed of 1°/min. The chemical structure of sample was examined using a Fourier transform infrared spectroscopy (FTIR; Bruker Vertex 80v, Ettlingen, Germany) with a spectral resolution of 1 cm^{-1} in reflection adsorption. The surface morphology of the cement sample was coated with gold using a JFC-1600 (JEOL, Tokyo, Japan) coater and observed under a field emission scanning electron microscope (SEM; JEOL JSM-7800F, JEOL Ltd., Tokyo, Japan) operated in the lower secondary electron image (LEI) mode at 1 kV of accelerating voltage after being dried with liquid CO_2 using a critical point dryer device (LADD 28000, LADD, Williston, VT, USA).

2.8. Diametral tensile strength

The diametral tensile strength (DTS) test was carried out using an EZ-Test machine (Shimadzu, Kyoto, Japan) at a loading rate of 0.5 mm/min. The strength value of each cement sample was calculated using the following relationship: the strength = $2P/\pi bw$, where P is the peak load (N), b is the diameter (mm), and w is the thickness (mm) of the sample. The maximal failure load was obtained from the recorded load-deflection curves. Ten repeated samples were tested at each time point.

2.9. Porosity

The measurement of the porosity was conducted using a gravimetric method based on Archimedes' method. In this method, since water was the setting medium, ethanol was used instead of water as the immersion liquid. The average value of the five measurements was taken as the porosity of the samples. First, the samples were dried in an oven at 120 °C for 2 h, and then the dry weight (W_{dry}) was measured. The sample was suspended in ethanol to fill out any pores and weighed as the suspended weight (W_{susp}). Afterwards, the saturated sample submerged in ethanol was taken out, followed by removing all the droplets gently from the surface, and then determining the saturated weight (W_{sat}). Thus, the apparent porosity of the cement sample was obtained by the following formula:

$$\text{Apparent porosity } (\%) = W_{sat} - W_{dry}/W_{sat} - W_{susp} \times 100\%$$

2.10. In vitro bioactivity

To evaluate in vitro bioactivity, the sample was soaked in an SBF solution with pH 7.4 at 37 °C, which corresponded to a sample surface-to-volume ratio of 0.1 cm^{-1}. The acellular, protein-free SBF solution with ionic composition similar to that of human blood plasma consisted of 7.9949 g sodium chloride (NaCl; J.T. Baker, Phillipsburg, NJ, USA), 0.3528 g sodium hydrogen carbonate ($NaHCO_3$; Showa), 0.2235 g potassium chloride (KCl; Showa), 0.178 g dipotassium hydrogen phosphate (K_2HPO_4; Showa), 0.305 g magnesium chloride hexahydrate ($MgCl_2{\cdot}6H_2O$; Showa), 0.2775 g calcium chloride ($CaCl_2$; Showa), and 0.071 g sodium sulfate anhydrous (Na_2SO_4; Showa) in 1000 mL of distilled H_2O and was buffered to pH 7.4 with hydrochloric acid (HCl; Shimada, Osaka, Japan) and trishydroxymethyl aminomethane ($(CH_2OH)_3CNH_2$; Acros, Morris Plains, NJ, USA). All chemicals used were reagent grade and used as received. In order to simulate the continuous circulation of physiological fluids in the body, continuous exchange of SBF (dynamic condition) may be a more efficient assay, which can more accurately precise in vitro bioactivity and degradation than static assays (lack of SBF exchange). The peristaltic pump had a feeding rate of 1 mL/min [31]. After soaking for a certain period of time (1 day, 1 month, 2 months, and 3 months), the sample was taken out from the vials for measurement of diametral tensile strength, or dried in an oven at 60 °C for the analysis of morphology, composition, porosity, and weight loss. To measure the weight loss, the dried samples were weighed using a four-digit balance (AE 240S, Mettler-Toledo AG, Greifensee, Switzerland) until a constant weight was reached before (day 0) and after soaking in SBF. Ten replicate samples were examined for each material investigated at each time point, except the 1-day group.

2.11. Cell culture

The biological function of bone cement was evaluated using the human osteoblast-like cell line MG63 (Hsinchu BCC 60279, Taiwan). The cells were suspended in Dulbecco's modified Eagle medium (DMEM; Gibco, Langley, OK, USA) containing 10% fetal bovine serum (FBS) (Gibco) and 1% penicillin/streptomycin solution (Gibco) in 5% CO_2 at 37 °C. Samples were sterilized by soaking in a 75% ethanol solution and exposure to UV light overnight before cell incubation.

2.11.1. Cell attachment and proliferation

MG63 cell suspensions at a density of 10^4 cells/mL were directly inoculated on each cement samples. The cells were cultured for 6, 12, and 24 h to assess attachment while cell proliferation was examined at days 3 and 7. After the established incubation period, cell viability was examined using the MTT (3-(4,5-dimethylthiazol-2-yl)-2,5-diphenyltetrazolium bromide; Sigma-Aldrich) assay, in which tetrazolium salt is reduced to formazan crystals by the mitochondrial dehydrogenase of living cells. Briefly, 3 h before the end of the incubation period, 200 μL of 0.5 mg/mL MTT solution in DMEM containing 1% penicillin/streptomycin and 200 μL of dimethylsulfoxide (DMSO; Sigma-Aldrich) were added to each well. The plates were then shaken until the formazan crystals had dissolved, and 100 μL of the solution from each well was transferred to a 96-well tissue-culture plate. Plates were read in a BioTek Epoch spectrophotometer (Winooski, VT, USA) at 563 nm. The results were reported in terms of absorbance. The results were obtained by six independent measurements.

2.11.2. Alkaline phosphatase activity

To evaluate the effect of hybrid cement on early cell differentiation, the alkaline phosphatase (ALP) activity assay was carried out using the TRACP & ALP assay kit (Takara, Shiga, Japan) according to the manufacturer's instructions. MG63 cells were seeded at a density of 5000 cells/well. ALP catalyzes the hydrolysis of the colorless organic phosphate ester substrate, *p*-nitrophenyl phosphate (pNPP), to *p*-nitrophenol, a yellow product, and phosphate. For the assay, after 7 and 14 days of incubation, the cells were washed with physiological saline (150 mM NaCl) and lysed in 50 μL of lysis buffer (1% NP40 in 150 mM NaCl). For measurement purposes, 50 μL of the substrate solution (20 mM Tris–HCl, 1 mM $MgCl_2$, 12.5 mM pNPP, pH = 9.5) was added to each well and allowed to react in the dark at 37 °C for 30 min. The reaction was stopped by the addition of 50 μL of 0.9 M NaOH and read at 405 nm using a BioTek Epoch microplate reader. Three independent measurements were made.

2.11.3. Calcium quantification

The mineralized matrix synthesis was analyzed using an Alizarin Red S staining method, which identifies calcium deposits. The cells (5000 per well) were seeded into 48-well culture dishes. After culture for 7 and 14 days, the cells were washed with phosphate buffer solution (PBS, pH 7.4) and fixed in 4% paraformaldehyde (Sigma-Aldrich) for 10 min at 4 °C. It was then stained for 10 min at room temperature in 0.5% Alizarin Red S (Sigma-Aldrich) in PBS. Cells were completely washed with PBS and then observed using an optical microscope (BH2-UMA; Olympus, Tokyo, Japan). To quantify matrix mineralization, the calcium mineral precipitate was destained by 10% cetylpyridinium chloride (Sigma-Aldrich) in PBS for 30 min at room temperature. The absorbance of Alizarin Red S extracts was measured at 562 nm using a BioTek Epoch microplate reader. Mean absorbance values were obtained from three independent experiments.

2.12. Antibacterial activity

The antibacterial activity of the set cement samples was evaluated using *E. coli* (ATCC 8739 Hsinchu, Taiwan) and *S. aureus* (ATCC 25923, Hsinchu, Taiwan). After mixing the powder with the liquid, the cement was directly placed in 48-well culture dish for 1 day to be hardened. Bacterial cultured on the cement-free dish was used as a negative control, and the $Ca(OH)_2$ cement was referred as a positive control. Calcium hydroxide has been widely used as an antibacterial agent in many clinical conditions such as in infected root canals [32]. Furthermore, it is also one of the setting products of calcium silicate cement. Thus, this may explain why calcium hydroxide was used as a positive control. $Ca(OH)_2$ cement (Showa) was prepared at a L/P of 0.3 mL/g. Before seeding the bacteria, samples were sterilized by soaking in a 75% ethanol solution and exposure to ultraviolet light for 2 h. After washing three times with PBS, the cement sample was cultured with 500 μL of the bacterial suspension (10^7 CFU/mL) in Bacto tryptic soy broth (Becton Dickinson, Sparks, MD, USA) for 3, 6, 12, 24, and 48 h culture time. Afterwards, the antibacterial activity of the samples was assessed by an Alamar Blue (Invitrogen, Grand Island, NY, USA) assay. At the end of the culture period, each well was filled with 500 μL of solution at a ratio of 1:10 of Alamar Blue to broth and incubated at 37 °C for 1 h. Subsequently, 150 μL of the solution from each well was transferred to a new 96-well plate and read at 570 nm with reference wavelength of 600 nm in a BioTek Epoch microplate reader. The bacteriostasis ratio (%) was calculated as follows: (absorbance of Alamar Blue obtained on the negative control–absorbance of Alamar Blue obtained on the other materials)/absorbance of Alamar Blue obtained on the negative control × 100% [10]. The results were obtained in triplicate. To observe morphology and the amount of bacteria on the sample surface, after 24 h of seeding, the samples were washed three times with PBS and fixed in 4% paraformaldehyde for 15 min. After dehydration for 15 min in each gradient of the ethanol series and drying overnight, the samples were coated with gold and observed by SEM.

2.13. ROS detection

Intracellular ROS production was examined using a cell-permeant fluorescent probe, 5-(and-6)-carboxy-2′,7′-dichlorodihydrofluorescein diacetate (carboxy-H2DCFDA (C400), ThermoFisher, Eugene, Oregon, USA), according to the manufacturer's guideline. A probe solution (5 mM) was prepared in 100% ethanol. 1 mL of bacteria was cultured in Bacto tryptic soy broth at a density of 10^7 CFU/mL for 1 day and then was loaded with 1 μL of C400 at a working concentration of 5 μM for 30 min in the dark. Bacterial cells were collected by centrifugation at 10,600 rpm for 1 min and washed by PBS. The dye penetrated cells freely and was then hydrolyzed by the intracellular esterases to deacetylated H2DCF and trapped inside the cells. The bacteria were then treated with the antibacterial agents including CTS, QTS, and COS solutions for 1 h. 10% H_2O_2 was used as a positive control [33], while a PBS solution without an antibacterial agent was considered a negative control. The formation of highly fluorescent DCF is due to the oxidation of deacetylated H2DCF by various ROS such as hydroxyl radicals, hydrogen peroxide, and superoxide anions [34]. After the reaction, 200 μL of the solution was transferred to a fresh 96-well microtiter plate and then detected using a CLARIOstar® high performance microplate reader (BMG Labtech, Offenburg, Germany) at an excitation wavelength of 488 nm and an emission wavelength of 525 nm. The intensity ratio of ROS generation was defined as the ratio of fluorescence intensity of the liquid examined after inoculation in the bacterial species to that of the negative control without liquid. At least six separate experiments were conducted on all tests.

2.14. Statistical analysis

One-way analysis of variance (ANOVA) was used to evaluate significant differences between means in the measurement data. Scheffe's multiple comparison test was used to determine the significance of the standard deviation in the measurement data for each sample under different experimental conditions. In all cases, at a p value of < 0.05, the results were considered to be statistically different.

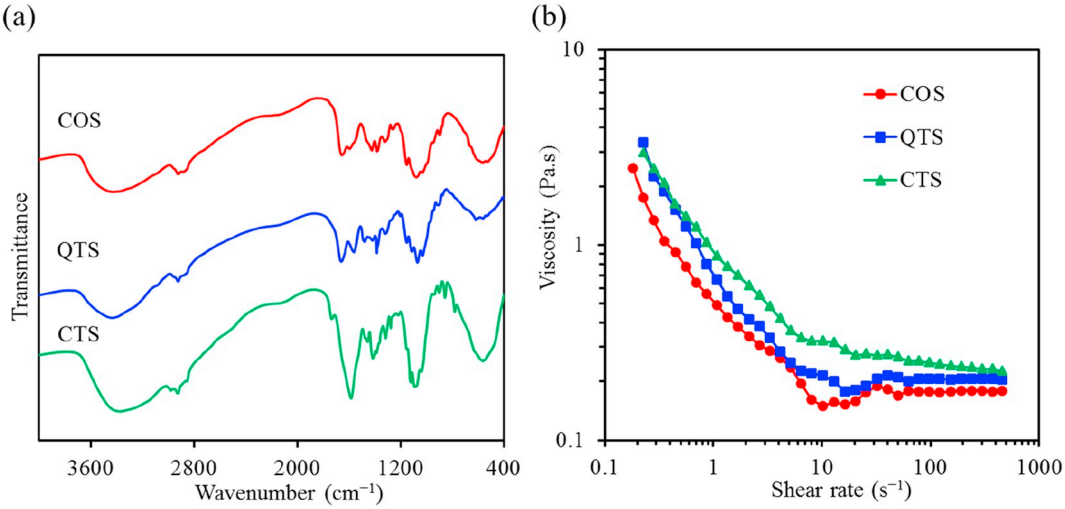

Fig. 1. (a) FTIR transmittance spectra and (b) the curves of viscosity versus shear rate for various chitosan samples.

3. Results

3.1. Properties of chitosan

The FTIR spectra of the three chitosan samples in transmission mode exhibited similar patterns to each other (Fig. 1a), which displayed an alkyl C—H stretching at 2856 and 2925 cm^{-1} [35] and saccharine structure involving C—N and C—O stretching at 1040–1152 cm^{-1} [36,37]. However, subtle differences were found in the extent of the substitution group. CTS was characterized by its amine NH_2 stretching vibration at 1584 cm^{-1} [36]. COS might be confirmed by the bands in the 1595 cm^{-1} and 1655 cm^{-1} related to NH_2 scissoring and C═O stretching peaks [38], respectively. The synthesis of QTS could be verified by the presence of the methyl band at 1478 cm^{-1} [38].

On the other hand, at the same 1% concentration, the relationship between the apparent viscosity and shear rate of the three chitosan solutions is shown in Fig. 1b. The viscosity of the chitosan solution decreased as the shear rate increased and then reached a steady state. It was observed that the apparent viscosities of CTS, QTS, and COS were 0.24, 0.21, and 0.17 Pa·s at a shear rate of 100 s^{-1}, respectively. At shear rates > 400 s^{-1}, the viscosity of QTS was very close to CTS. The viscosity of COS was lower than CTS and QTS.

3.2. Handling properties of cement

3.2.1. Anti-washout property of cement

Fig. 2 shows the results of the washout resistance, which photographs were taken 60 min after the cement samples were placed in the water immediately after mixing. The CS control (Fig. 2a), CT01, CT05, QT05, and all COS groups (Fig. 2d) were completely disrupted. However, when the used concentration of CTS and QTS was 1% or higher, the corresponding CT1 (Fig. 2b) and QT1 (Fig. 2c) cement samples were resistant to washout and revealed a stable shape without remarkable disintegration.

3.2.2. Setting time

After mixing with water, the setting time of the CS control cement was 18 min (Table 1). When the proportion of the additive component in the cement was altered, the setting time of the hybrid cement also changed. When the CaSi powder was mixed with the CTS, QTS or COS liquid, the setting time of the hybrid cement became longer as the amount of the liquid additive increased, indicating a significantly difference ($p < 0.05$). For example, cement prepared from 0.5 wt% CTS (CT05) or 5 wt% QTS (QT5) had a setting time of 37 or 41 min, respectively, which was significantly ($p < 0.05$) higher than the CS control. Similarly, as a 10% COS in the liquid phase, the setting time of the cement significantly ($p < 0.05$) was prolonged by up to 41 min. Interestingly, at the same concentration of 1%, different types of chitosan resulted in significantly different setting time. The CT1, QT1, and CO1 cements had the setting time of 100, 34, and 20 min, respectively.

3.2.3. pH value

Table 1 lists the pH values of the cement samples after mixing. The pH of the CS control was approximately 11.7, which was significantly ($p < 0.05$) higher than those of the CTS groups ranging from 10.5 to 10.6. It can be clearly seen that as the concentration increased, the

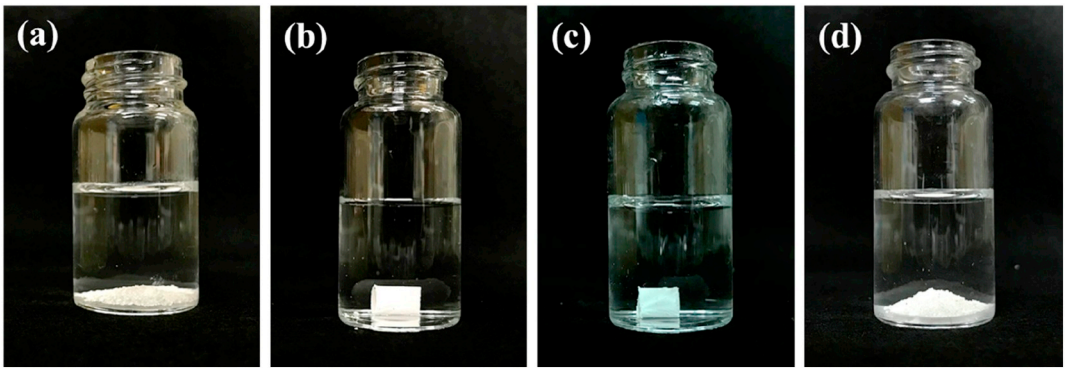

Fig. 2. Anti-washout properties of (a) the control, (b) CT1, (c) QT1, and (d) CO10 bone cements. Immediately after mixing, the cement bulks was immersed in water. The picture was taken 1 h later.

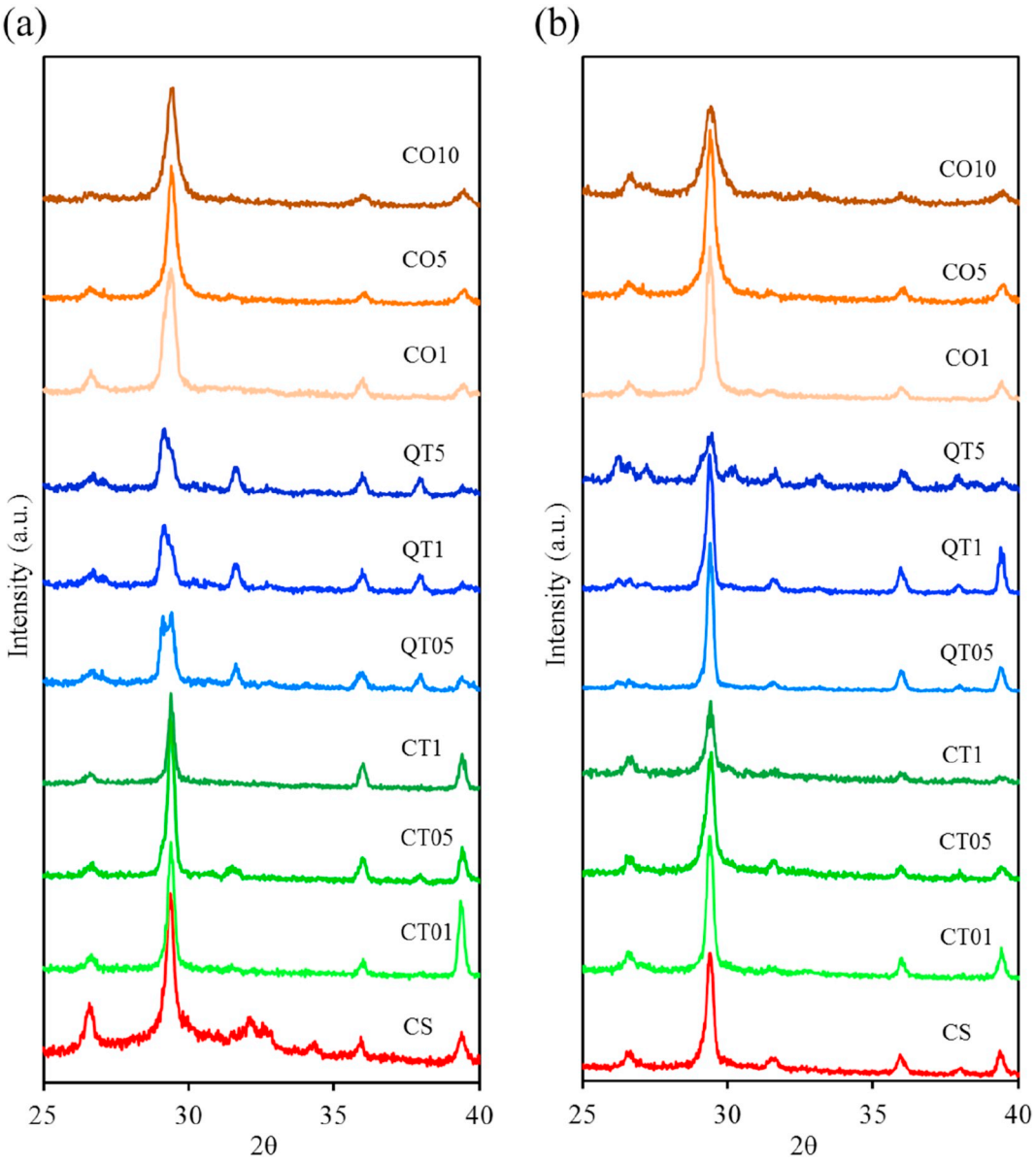

Fig. 3. XRD patterns of various bone cements (a) before and (b) after soaking in SBF for 1 day.

cement pH of the QTS group slightly increased from 11.6 to 11.9, which was equivalent to the control. Regarding the COS group, the pH decreased with increase in the concentration, indicating a range of 11.4–11.1.

3.3. In vitro bioactivity

3.3.1. Phase composition

The XRD patterns of all the hardened cements indicate a sharp diffraction peak at 2θ = 29.4°, which corresponded to the calcium silicate hydrate (C—S—H) phase structure overlapping with calcite ($CaCO_3$) because of the hydration reaction, as shown in Fig. 3a. In addition, there was the incompletely reacted inorganic component phase of β-Ca_2SiO_4 at 2θ between 32 and 34°. A diffraction peak at 2θ = 26.6° was ascribed to the $CaSiO_3$ (wollastonite) phase. When compared with the control cement, it can be inferred that the peak intensity of C—S—H, β-Ca_2SiO_4 and $CaSiO_3$ could be slightly lowered due to the presence of amorphous chitosan material. After soaking in SBF for 1 day, the resulting XRD patterns were clear to see that the intensity of the β-Ca_2SiO_4 phase in the CS control was reduced (Fig. 3b), which may be due to the dissolution of this phase or the precipitation of amorphous precipitate on the cement surface. Except when a higher concentration of liquid phase was used, the peak intensity decreased at 2θ = 29.4°, and the diffraction patterns of all hybrid cements were similar to those of the control cement.

Basically, the FTIR spectra (Fig. 4a) of all cement samples before soaking in SBF were very similar to each other because of the small amount of chitosan liquid, consistent with the XRD trend. For example, the CS control had a broad IR absorption band of 1100 to 1400 cm^{-1} due to asymmetric stretching of Si—O—Si and formation of Si—O—Ca bonds [9]. The band between 740 and 850 cm^{-1} was assigned to the stretching mode of $CaCO_3$ and the symmetric stretching vibration of Si—O—Si [39]. The Si—O—Si bending band at around 590–660 cm^{-1} indicated the formation of the C—S—H structure [40]. After soaking for 1 day in SBF, the changes in the FTIR spectra of cements (Fig. 4b) were similar to those shown by XRD. However, the band at 740–850 cm^{-1} is weaker, while the band at 560–630 cm^{-1} was sharp, which can be possibly due to the P—O bending vibration of the PO_4 unit [41].

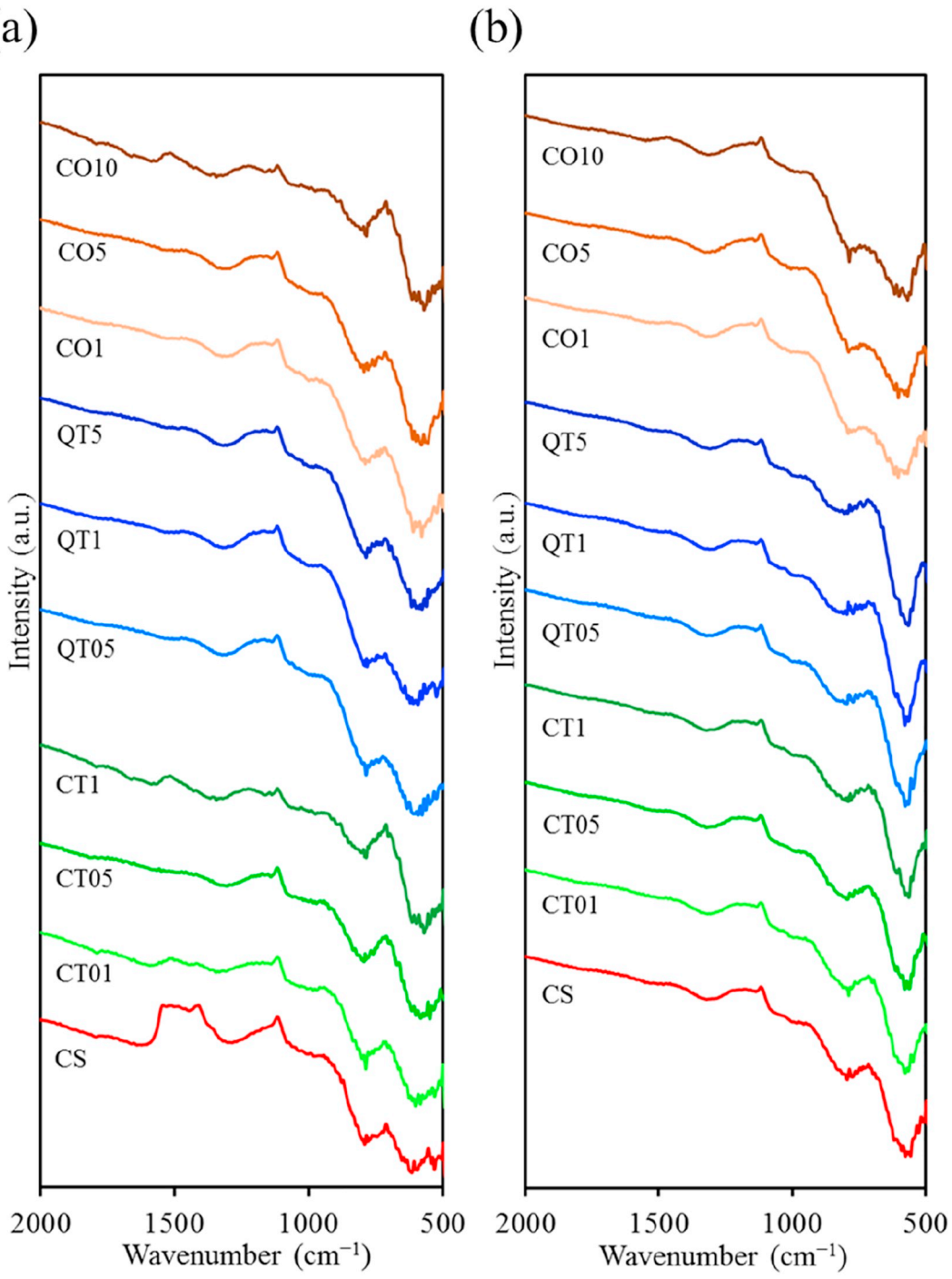

Fig. 4. FTIR spectra of the various bone cements (a) before and (b) after soaking in SBF for 1 day.

3.3.2. Morphology

The control cement consisted of entangled particles and appeared several pores (Fig. 5a). By contrast, when chitosan was added to the control, the hybrid cement became a more heterogeneous structure, exposing the polymer dense layer because of the viscous bonding between the particles (Fig. 5b–d). Broad face SEM micrographs of the cements after soaking in SBF for 1 day are shown in Fig. 6. Spherical precipitates were visible on the surface of the CS control. Similarly, all hybrid cements also formed spherules of approximately 1 μ in size, indicating a strong tendency to "attract" apatite precipitates onto their surfaces. To further confirm that the observed precipitates were apatite formed from an SBF solution, SEM/EDS analysis was performed on the 1-day-soaked samples. The Ca/P ratios of the soaked cement surfaces were between 1.7 and 2.8. Interestingly, the Ca/P ratio increased with increasing CTS content in the hybrid cement, which may be due to the water insolubility of the CTS. The QTS groups had the Ca/P ratio of about 2.3, which was higher than the CS control (1.8). In the case of COS, a higher concentration resulted in a higher Ca/P ratio of the spherical precipitates. After soaking the cement sample for 90 days (Fig. 7), the apatite spherules became lager than that formed on the 1-day sample.

3.3.3. Diametral tensile strength

Table 1 also shows that the set control cement had a DTS of 2.5 MPa. Interestingly, the incorporation of various chitosan as a liquid into the CS control slightly increased the strength. For the CTS group,

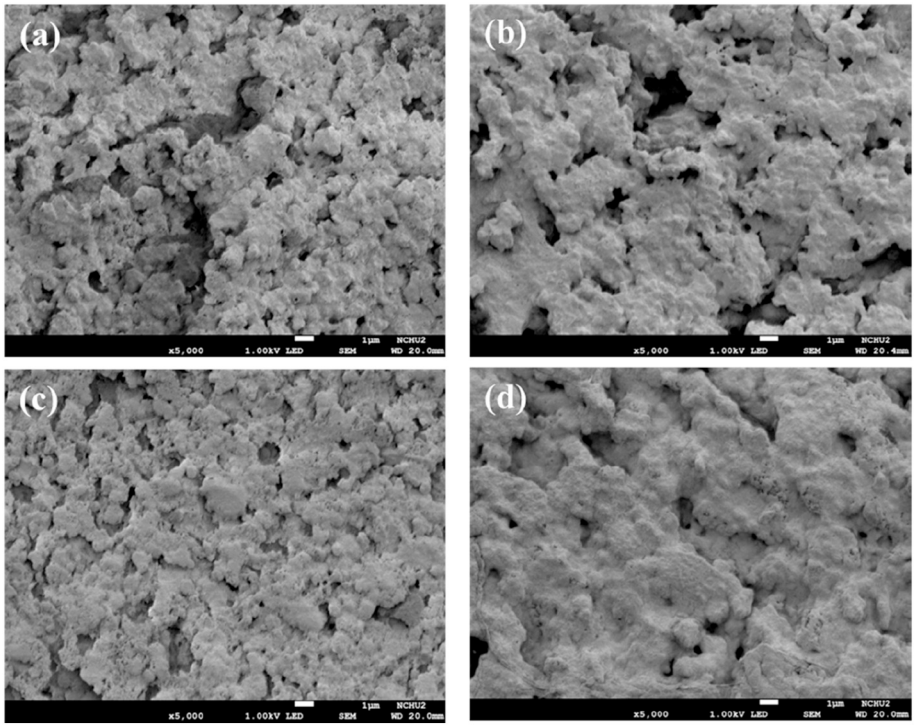

Fig. 5. SEM micrographs of (a) CS control, (b) CT1, (c) QT5, and (d) CO10 bone cements.

DTS values averaged 3.1, 3.1, and 3.4 MPa on average for concentrations of 0.1, 0.5, and 1%, respectively. When 0.5, 1, and 5% QTS was added to the CS control, the strength values were changed to 3.2, 3.3, and 3.5 MPa, indicating a significant difference ($p < 0.05$) from the control. Similarly, the strengths of 1, 5, and 10% COS were 2.7, 2.9, and 3.1 MPa, respectively. On the other hand, the porosity values of all cements were in the range of 16–18%, indicating no significant difference ($p > 0.05$) (Table 1).

The relationship between the liquid concentration and the diametral tensile strength of the cement before and after soaking in an SBF solution for 30, 60, and 90 days is shown in Fig. 8. Generally, regardless of the type of the hybrid cements, the strength values gradually reduced as the SBF soaking time increase. For example, after 90 days of soaking, the strength value of the CS control became 1.6 MPa, which was significantly lower ($p < 0.05$) than the original 2.5 MPa at day 0. For the 1% CTS-containing cement sample, the strength changed from 3.4 MPa to 2.0 MPa after 90 days of soaking (Fig. 8a). The strength values of QTS (Fig. 8b) and COS (Fig. 8c) cement groups showed the same trend as the CTS group (Fig. 8a). The strength values of QT1 were 3.1, 2.3, and 1.9 MPa after 30-, 60-, and 90-day soaking, respectively, while CO1 had the strength of 2.5, 1.8, and 1.6 MPa, respectively. It is worthy to note that the highest content (CT1, QT5, and CO10) of the three hybrid cement samples was higher than the CS control after 90 days of soaking.

3.3.4. Porosity and weight loss

As shown in Fig. 9, the porosity of all cement samples increased with increasing immersion time in SBF. This showed an inverse correlation to the strength trend. After 90-day soaking, the porosity value increased from an initial porosity of approximately 17% to a range of 45–52%, indicating a significant difference ($p < 0.05$). The degradation of all cement samples were also evaluated by their weight changes in SBF (Fig. 10). After soaking for 30 days, all cements displayed a small amount of weight loss (~2%), regardless of the type and concentration of chitosan. After 60 days of soaking, weight loss of all cement samples increased slightly. Interestingly, the extended 90-day soaking time did not seem to reduce weight.

3.4. In vitro osteogenesis

3.4.1. Cell attachment

In order to evaluate the effect of the type and concentration of chitosan in hybrid cements on osteogenic activity in vitro, the biological function of MG63 cells cultured on the surfaces of the cements were studied. Fig. 11a shows that higher CTS, QTS, and COS concentrations in the hybrid cement lead to lower cell growth. At the culture interval, the attachment of MG63 cells cultured on CT01, QT05, and COS1 was comparable to that of the CS control.

3.4.2. Cell proliferation

After 3 and 7 days of culture, the absorbance value increased with the increase of the culture time, revealing an increasing number of viable cells (Fig. 11b). However, compared with the CS control, the liquid phase of the cement caused a significant ($p < 0.05$) reduction in cell proliferation on the cement surface. As demonstrated in cell attachment, CT1 cement had the lower proliferation compared to the other two hybrid cements (QT1 and CO1) at the same 1 wt% concentration. On day 7, compared to the CS control, CT1's metabolic activity was significant reduced by 60% ($p < 0.05$), while the QT1 and CO1 cement were reduced by 40% and 15%, respectively.

3.4.3. ALP activity

Intracellular ALP levels were examined to assess the early differentiation activity of MG63 cells after 7 and 14 days of culture, as shown in Fig. 11c. At all culture time points, as the CTS, QTS, or COS content in the hybrid cement increased, the ALP level decreased, which was also significantly ($p < 0.05$) lower than that of MG63 cells cultured on the surface of the CS control. As the culture time was extended from 7 days to 14 days, all cements exhibited an increased amount of ALP. Interestingly, the ALP level of QT1 was higher than that of CT1.

3.4.4. Mineralization

To further understand the effect of different types and concentrations of cements on cell mineralization, extracellular matrix mineralization was quantified by Alizarin Red S assay. The amount of Ca

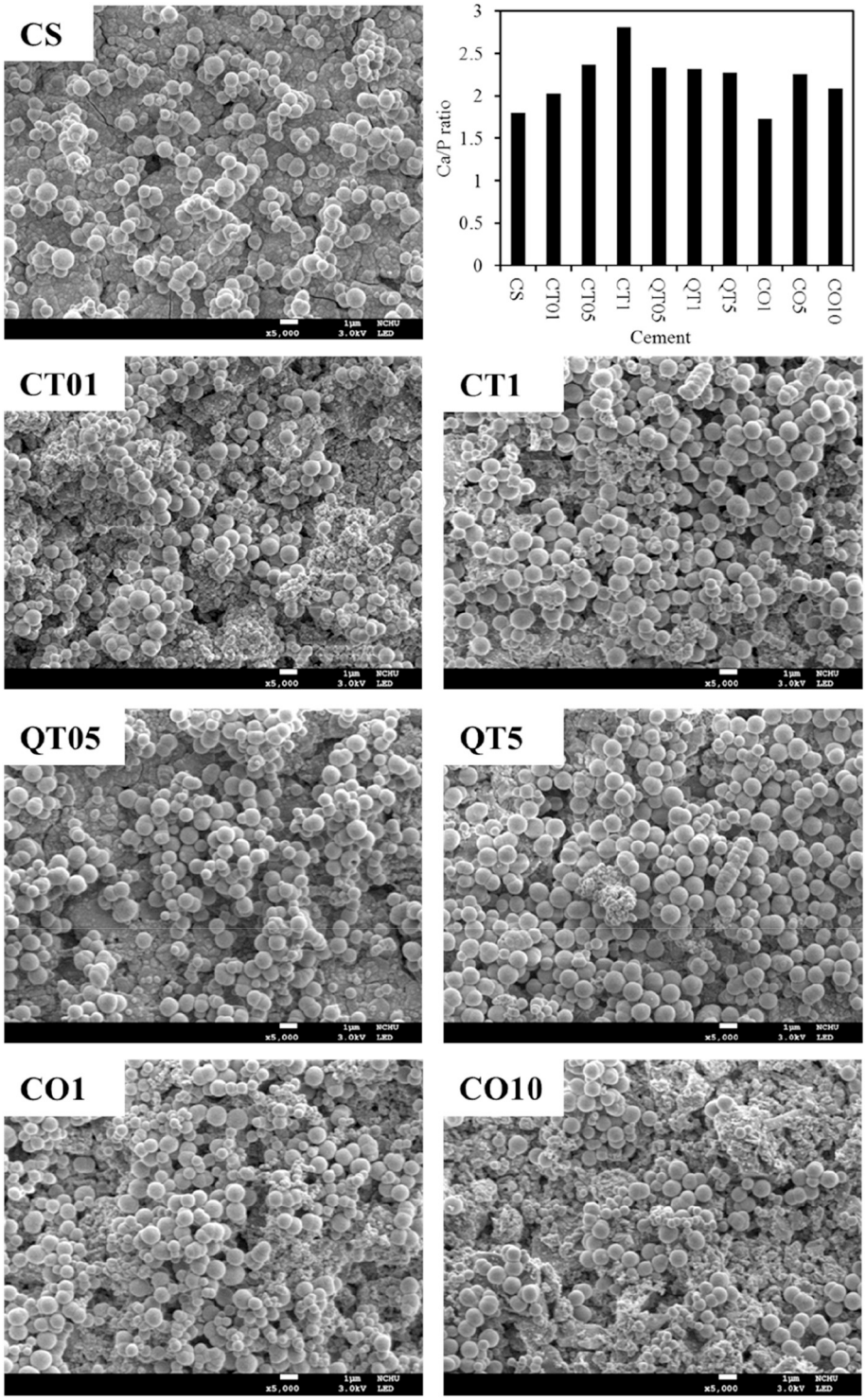

Fig. 6. SEM micrographs and Ca/P ratio of the various cement samples after soaking in SBF for 1 day.

deposit increased with increasing culture time (Fig. 11d). Similar to the findings of ALP activity, the greater chitosan concentration in the hybrid cement samples gave rise to the lower Ca amount on the cement surfaces, indicating an inverse concentration-mineralization correlation. After 7 and 14 days of culture, the Ca deposit contents of MG63 cells seeded on the surfaces of hybrid cements were lower than those of the CS control. Regarding the highest concentration of each chitosan used, CO10 cement showed higher Ca deposit than CT1 and QT5 cement, and the expression of the latter two was similar.

3.5. Antibacterial activity

3.5.1. Bacteriostasis ratio

To clarify the antibacterial efficacy of the hybrid cements, the Alamar Blue viability assay was used to examine the number of viable *E. coli* (Fig. 12a) and *S. aureus* (Fig. 12b) with and without contact with cement samples at different times, and then calculate the bacteriostasis ratio (%). It was clearly seen that a component-dependent bacteriostasis ratio for adherent *E. coli* and *S. aureus* bacteria was observed. Not surprisingly, the $Ca(OH)_2$ cement almost exerted a complete

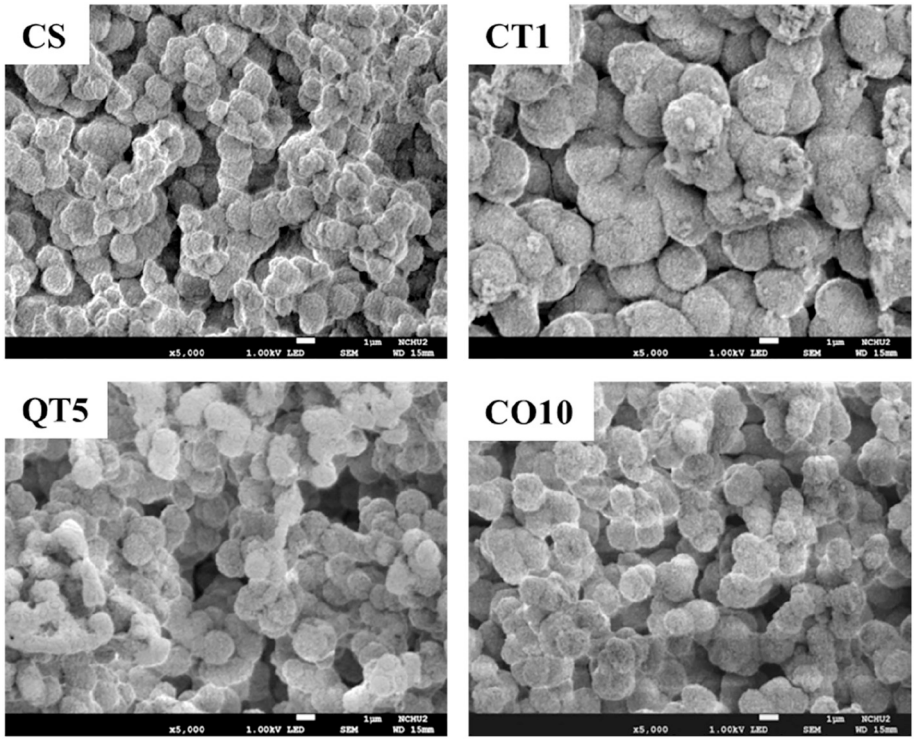

Fig. 7. SEM micrographs of various cement samples after soaking in SBF for 3 months.

bacteriostatic effect on bacterial species at all culture time points. The bacteriostasis ratio of CS control was 30 to 56% against *E. coli* during culture interval. At all culture time points, the bacteriostasis ratio of cement with higher chitosan content cements was significantly ($p < 0.05$) higher than that of lower content cement. At 3 h of seeding, 1% CTS, 5% QTS, and 10% COS cement samples almost completely killed *E. coli*, while the CS control had a reduction efficacy of only 56%. For longer time points such as 48 h, the bacteriostasis ratios decreased slightly. The 1% CTS, 5% QTS, and 10% COS cement samples revealed values of 87%, 73%, and 62%, respectively, but indicating significantly ($p < 0.05$) higher than the CS control of 30%. At the same 1% concentration, it was evident that the COS-containing cement resulted in the worst bacteriostasis ratio of the three chitosan biomolecules. In contrast, CTS had greater antibacterial efficacy than other biomolecules.

In the case of *S. aureus*, at first glance, the data shown in Fig. 12b pointed out a similarly prominent trend, namely that the higher the chitosan content in the cement, the higher the bacteriostasis ratio at all culture time points. The bacteriostasis ratios of hybrid cements prepared with the highest concentration of each chitosan biomolecule were comparable to those of the $Ca(OH)_2$ cement, indicating their bacteriostasis ratio was about 90%. By adding these chitosan biomolecules, the antibacterial activity of the CS control was significantly improved.

3.5.2. Bacterial adhesion

To further elucidate the antibacterial activity of all hybrid cements, the bacterial adhesion on the cement surface was observed by SEM after seeding *E. coli* and *S. aureus* for 24 h, as shown in Fig. 13. On the surface of the CS control, the rod-shaped Gram-negative *E. coli* colonies grew well, while the number of *E. coli* bacteria on the hybrid cements decreased noticeably (Fig. 13a). Similarly, spherical Gram-positive *S. aureus* bacteria on the CS control surface aggregated into grape-like colonies (Fig. 13b). Few *S. aureus* adhered to the CT1, QT5, and CO10 cement surfaces.

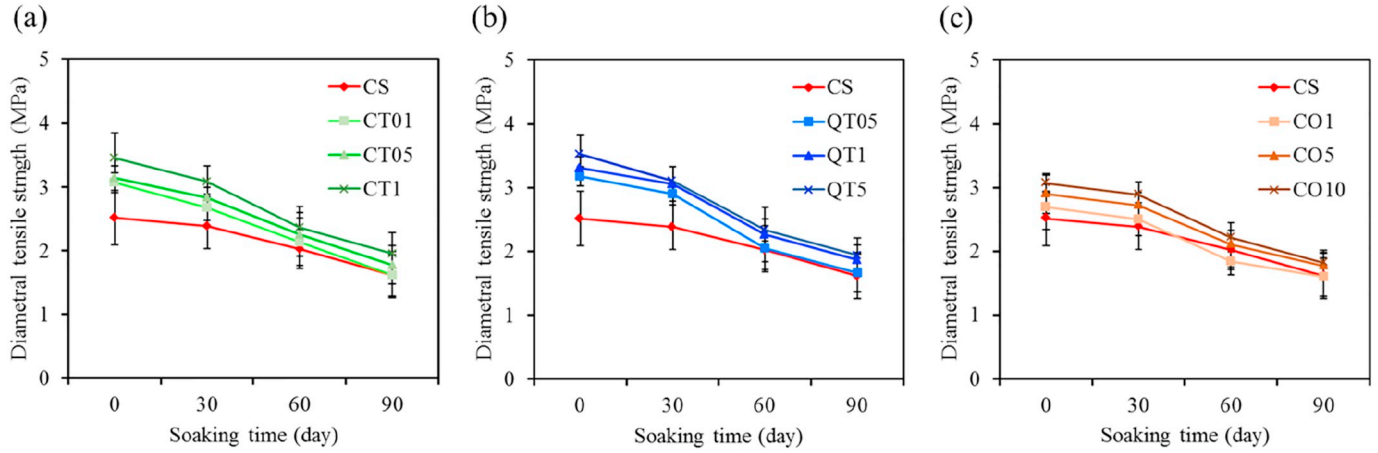

Fig. 8. Diametral tensile strength of the calcium silicate bone cements with (a) CTS, (b) QTS, and (c) COS before and after soaking in an SBF solution for different time points.

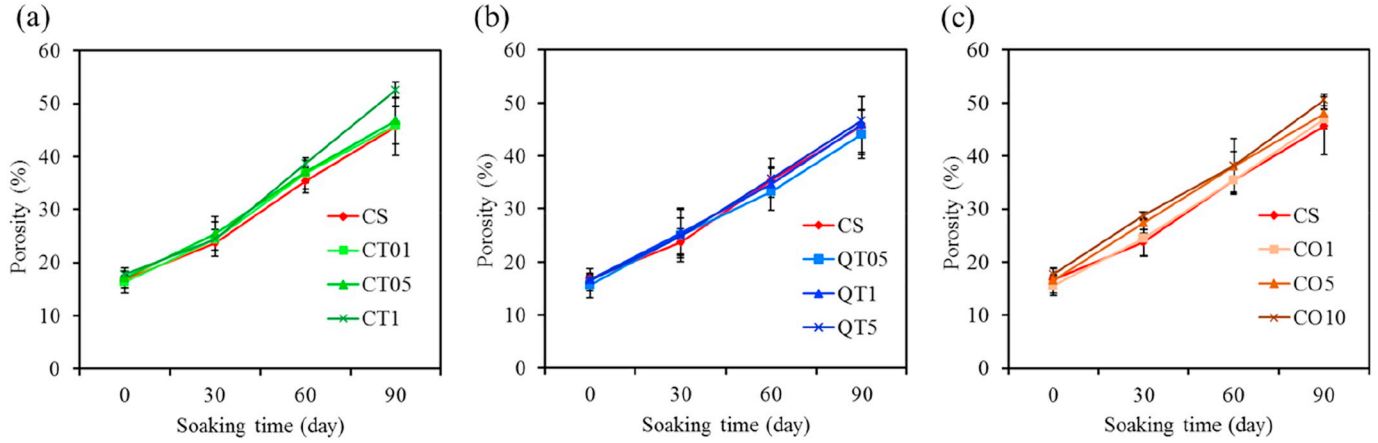

Fig. 9. Porosity of the calcium silicate bone cements with (a) CTS, (b) QTS, and (c) COS before and after soaking in an SBF solution for different time points.

3.6. ROS production

To further reveal the antibacterial mechanism of different chitosan materials, the ROS produced by bacteria were evaluated. In the absence of bacterial seeding, the fluorescence intensity of the C400 probe in the chitosan liquid used was quantified as a blank test. As expected, due to the lack of bacteria, the intensity of the blank test in all tested agents maintained a constant fluorescence intensity value (not shown), confirming that the antibacterial agents itself did not cause the ROS generation. Fig. 14 shows that the degree of ROS production in the two bacterial strains caused by 10 wt% H_2O_2 was much higher than that obtained from the other test agents. It is worth noting that exposure of various chitosan liquids to *E. coli* or *S. aureus* bacteria remarkably resulted in a concentration-dependent increase in intracellular ROS. Compared with the medium control without this agent, a low concentration of CTS (such as 0.1%) could lead to a 7-fold increase. Similarly, incubation with 1% QTS evoked a significant increase, which was 8-fold against *E.coli* and about 9-fold against *S. aureus*. In addition, the ROS production followed the order of CTS > QTS > COS at the same 1% concentration, regardless of the bacterial species. Moreover, 1% CTS, 5% QTS, and 10% COS had similar ROS production, which was in good accordance with the antibacterial activity.

4. Discussion

Bone tissue repair and regeneration at infected areas with impaired osteogenesis is a major clinical problem. In addition, with the emergence of antibiotic resistance in microorganisms, the incorporation of antimicrobial agents into bone grafts has attracted widespread interest. Despite the continuous development of various commercial cement products, such as CPC and CaSi-based cement, the development of new bone cements with antibacterial and osteogenic activity for clinical use has become increasingly important. Recent efforts in the development of antibacterial bone cement are encouraging, but there are still many concerns regarding the optimization of the properties of bone repair material. To achieve this goal, many studies have focused on the preparation of novel bone cements by incorporating additives with unique properties in cements [8,42]. It is believed that additives in powder or liquid form may adversely or positively affect the performance of bone cement [28,43,44]. In this study, by varying the type and concentration of chitosan biomolecules, compared with the individual components, the properties of the hybrid cement produced would change accordingly, thereby obtaining unique properties. For example, the presence of chitosan improved brittleness and strength of ceramic [1,20]. Because CTS has limited solubility even when dissolved in an acidic solution, three low concentrations (0.1, 0.5, and 1 wt%) were used in this study. Low viscosity water-dissolvable COS can be prepared at higher concentrations, including 1, 5, and 10% by weight. Among these three types of biomolecules, in order to compare the concentration effect, water-dissolvable QTS with a concentration of 0.5, 1, and 5 wt% was used, and its viscosity was between QTS and COS. Typically, higher molecular weight chitosan results in higher viscosity based on the Mark-Houwink relation [45]. Commercial COS with a molecular weight of < 5 kDa can be used to explain the lower viscosity in comparison with the other two molecules. Zou et al. described that, QTS and COS, as hydrolysis products of CTS, have better solubility and lower viscosity under physiological conditions because of the shorter chain lengths and/or free amino groups of D-glucosamine units [46].

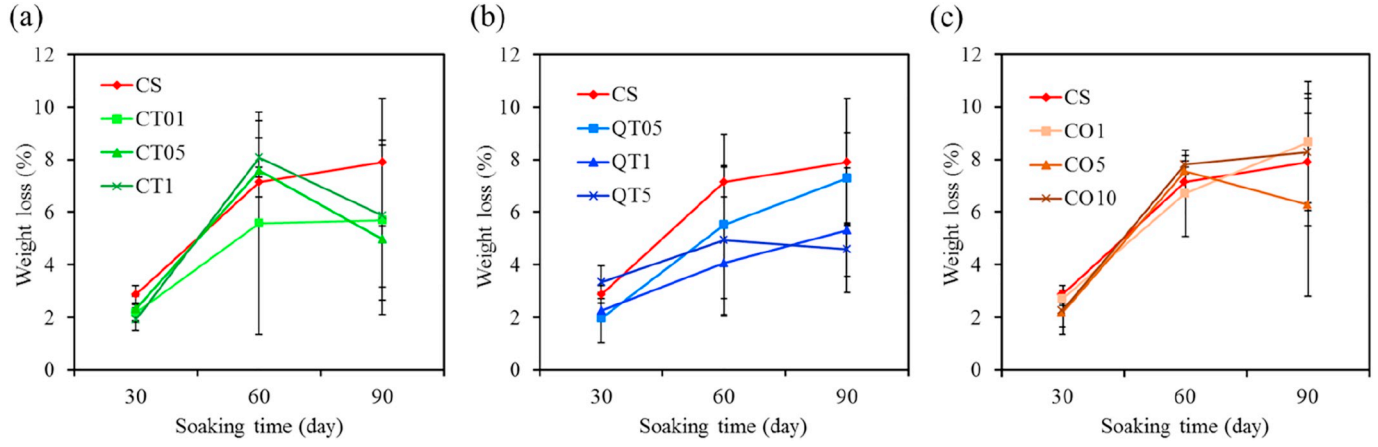

Fig. 10. Weight loss of the calcium silicate bone cements with (a) CTS, (b) QTS, and (c) COS before and after soaking in an SBF solution for different time points.

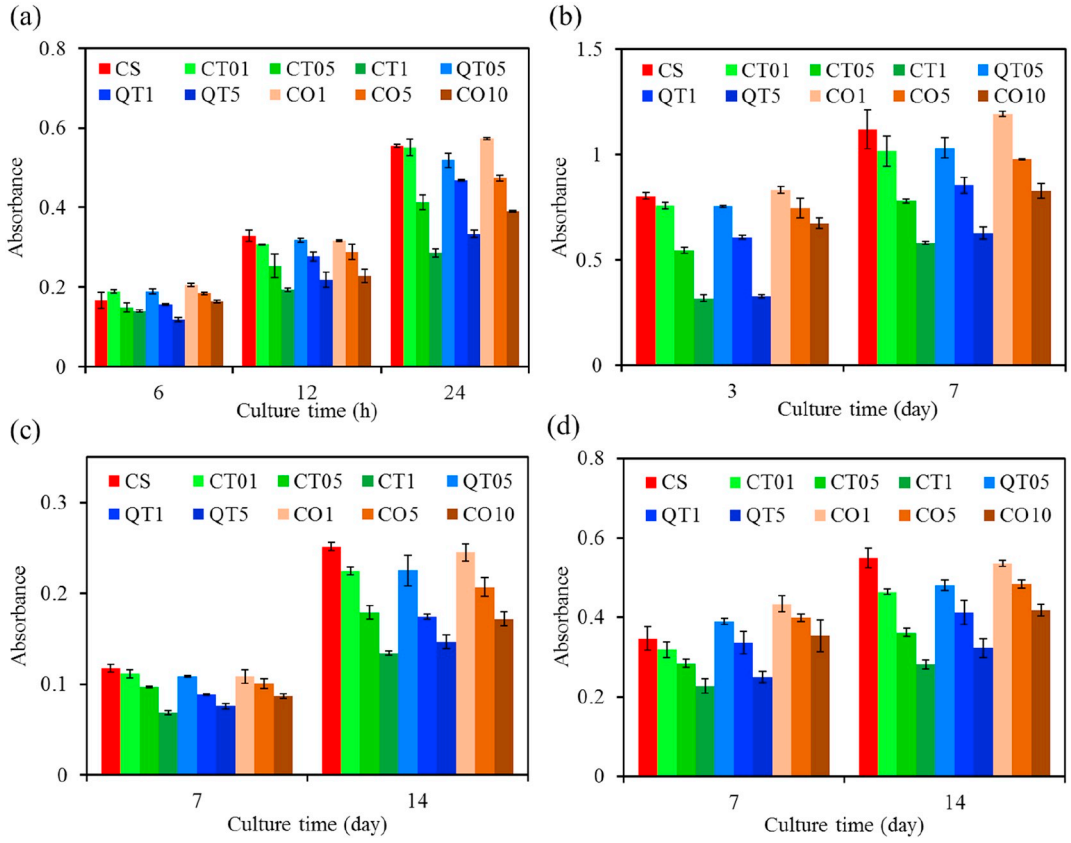

Fig. 11. (a) Attachment, (b) proliferation, (c) ALP activity, and (d) matrix mineralization of MG63 cells cultured on various cement surfaces at various culture time-points.

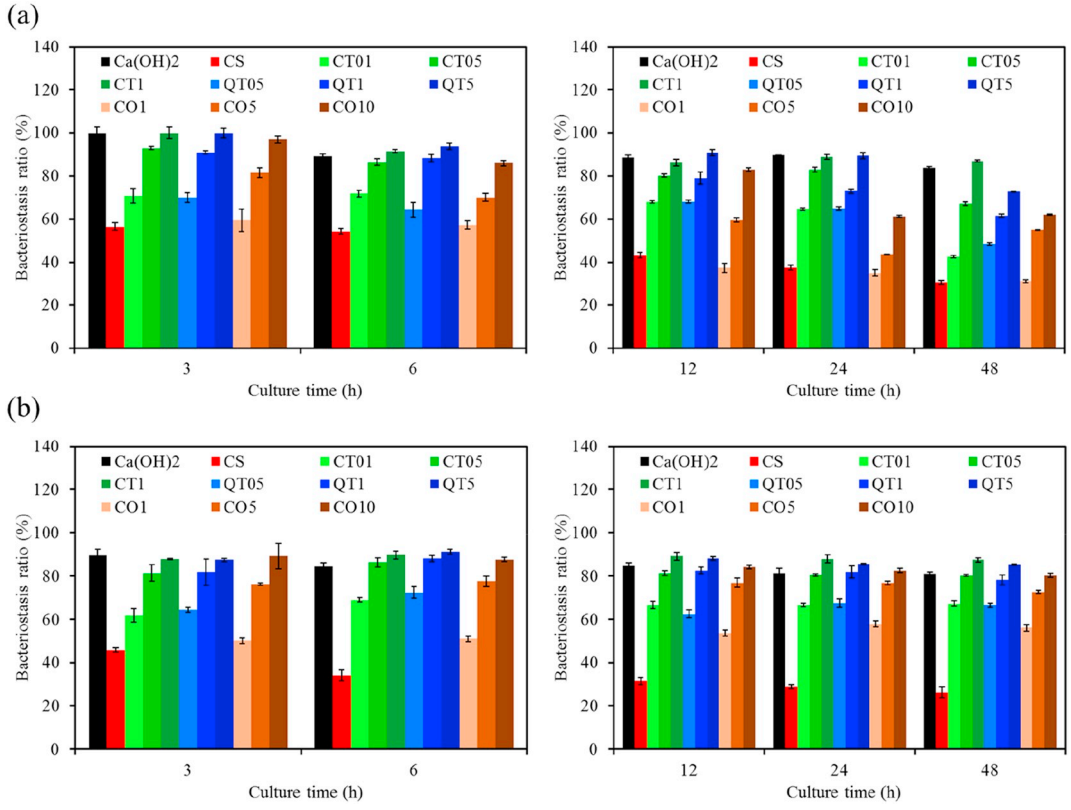

Fig. 12. Bacteriostasis ratio (%) of various cements after (a) *E. coli* or (b) *S. aureus* culture in contact with the cements at short-time and long-time points.

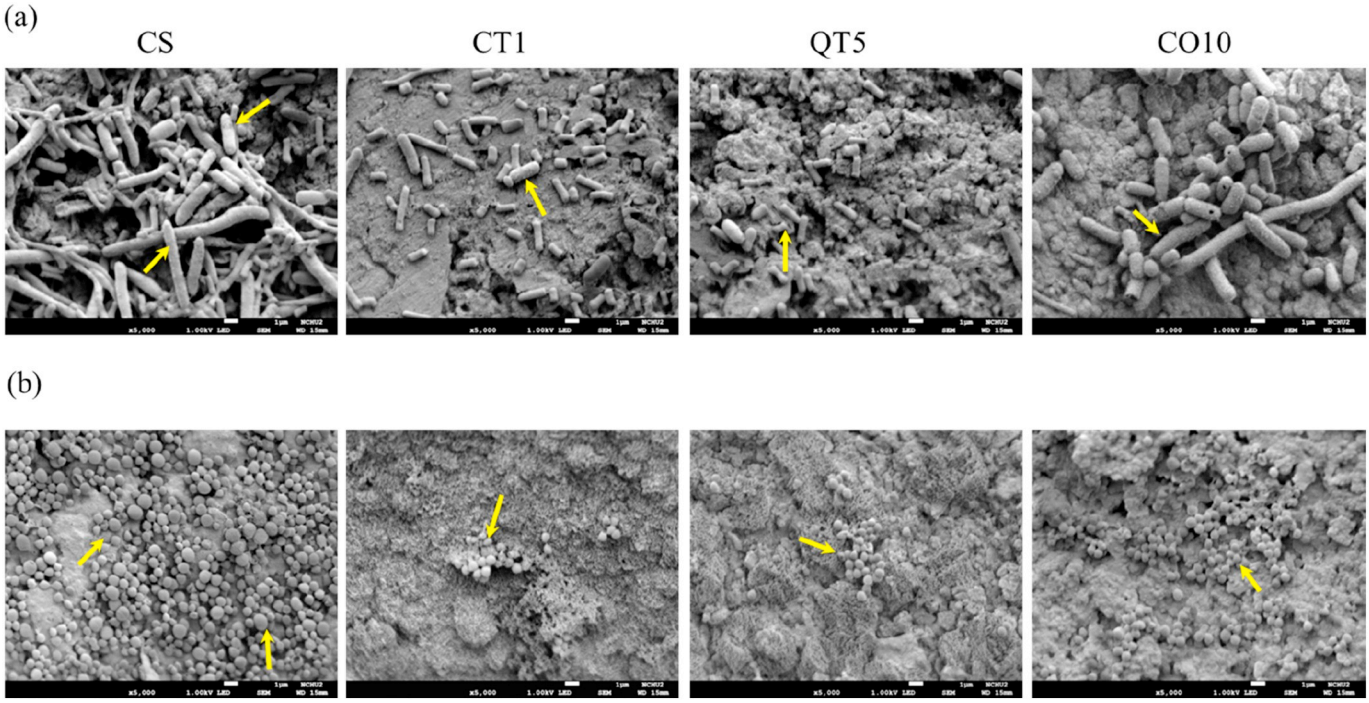

Fig. 13. SEM images of (a) *E. coli* and (b) *S. aureus* bacterial adhesion on the surfaces of CS, CT1, QT5, and CO10 cements after culture for 24 h. The arrows indicate the presence of the bacteria.

For the clinical need, ideal bone cement should have the merits of handling properties allowing for minimally invasive delivery and preventing from the disintegration during implantation [5]. When cement comes into contact with physiological fluids in the body or bleeding occurs, it is difficult to achieve complete hemostasis, so the washout phenomena of implanted cement takes place [47]. If the implanted cement does not have sufficient washout resistance (or viscosity) for body fluids, it is difficult to maintain the original grafted shape of the cement at the site of bone defect. Against this background of insufficient handling properties often encountered in ceramic cements, one of the current purposes was to improve shortcomings of today's materials by synergistically combining bioactive calcium silicate with viscous chitosan as a cohesion promoter. As a result, like the unmodified CS control, CT01, CT05, QT05, and all COS-containing cements rapidly decomposed into powder after soaking in water. The addition of these liquids did not improve the washout-resistant ability of the CS control. Contrary to the findings, CT1, QT1, and QT5 cements had the ability to resist water washout, possibly due to effective fuse of the particle together, just like glue. Although the detailed mechanism of the anti-washout ability of CaSi hybrid cements containing ≥1 wt% CTS (or QTS) has not yet been fully clarified, the enhancement in anti-washout properties may be attributed to viscous properties, as confirmed by the results of rheometer. This meant that chitosan with high viscosity and proper concentration could promote the washout resistance of ceramic cement. As mentioned previously, QTS had a similar viscosity to CTS and was higher than COS at the same 1% concentration. Therefore, the ability of gelling agents (such as viscous CTS and QTS) to impart viscous flow when wet and then firm the cement particles can transform CS control cement into a more anti-washout paste. Tappa et al. have reported that the addition of 10% chitosan lactate solution to CPC cause no disintegration because of its cohesive nature [48]. Physical reactions may inhibit the penetration of cement paste by liquids such as water, which is considered to be the cause of the cement washout properties [43,49,50]. But the inhibition behavior prolonged the setting reaction. Duarte et al. have utilized propylene glycol as an antiwashout promoter to improve the handling properties of CaSi-based mineral trioxide aggregate (MTA) Angelus, and found it prolonged the setting time in a dose-dependent fashion [51].

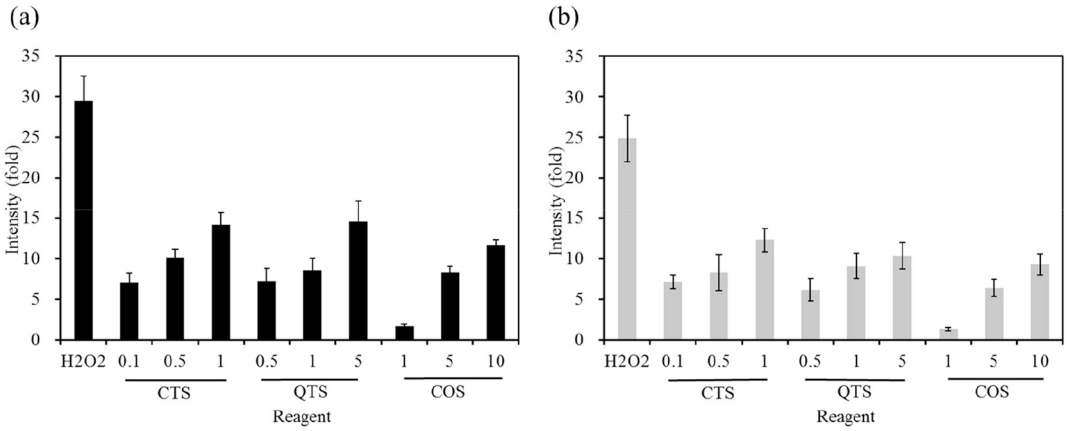

Fig. 14. The ROS production within the (a) *E. coli* and (b) *S. aureus* bacteria treated with the different concentrations and types of chitosan.

Setting time is an important factor in evaluating handling properties of the bone cement. Bone cement with long setting time cannot maintain shape and support stress during filling, which may cause clinical problems [5]. The recommended setting time is about 15 min for injectable bone cements [3]. In the current work, when water was used as the liquid phase, the setting time of the control cement was 18 min. In contrast, depending on the concentration and type used, the use of CTS, QTS, or COS liquid could prolong the setting time of the hybrid cements to 19–100 min. The higher the concentration of chitosan, the longer setting time of the hybrid cement was. It is worthy of noting that at the same concentration of 1 wt%, the setting times of CT1, QT1, and CO1 cements were 100, 34, and 20 min, respectively, which proved the hardening extension of the order CTS > QTS > COS. The resulting hardening properties of the new hybrid cements are the combination between the progressive hardening caused by the main CaSi ceramic reactants and the progressive complex reaction of the organic chitosan phase with water [43]. The latter can be explained by the fact that the side chains of the three CTS, QTS, and COS molecules have one amino group and one hydroxyl group. On the other hand, the currently used CaSi powders were positively charge Zeta potentials [52], and chitosan was positively-charged. Excessive polycations may disrupt the balance of the components in the cement, leading to a very slow setting processes [53,54]. In addition, the differences in setting time of the three chitosan biomolecules can be interpreted by different viscosities. Water-soluble COS molecules have a low viscosity [19], so the addition of low-concentration COS did not increase the setting time of the CS control. However, higher concentrations of up to 10% apparently prolonged the setting time of the CS control, which has been reported in an earlier study [44]. Lin et al. also found that 1.0 wt% water-soluble carboxymethyl chitosan extended the setting time of tricalcium silicate bone, despite its excellent anti-washout ability [53]. Hence, high viscosity CTS was expected to have a negative impact on the setting time of the hybrid cement.

Bone cement can be used to stimulate bone healing and fill bone defects. It is believed that the assessment of in vitro activity is an important first step before evaluating the in vivo behavior of cement. The in vitro bioactivity (or biodegradation) behavior of the various cement samples in an SBF solution was evaluated by examining changes in phase composition, morphology, diametral tensile strength, and weight loss. Before soaking in SBF, it is reasonable to find the similar phase composition for all cements because the chitosan additive was an amorphous phase [55]. Indeed, the diffraction intensities of the hybrid cements resulted mainly from the hydration product of C—S—H. Panahi et al. have suggested that the incorporation of chitosan in the CaSi cement composite inhibited the growth of C—S—H phase [54]. The increasing concentration of chitosan molecules made the diffraction peaks of CaSi gradually reduced. In addition, the film-forming capacity of chitosan can be used as glue for calcium silicate particles to form a smooth morphology [7].

When soaked in SBF for 1 day, the surface morphology of all hybrid cement samples was also similar to the CS control. The precipitated spherules have been identified as apatite in this and other studies [44,56]. Kim et al. have reported the formation of an amorphous calcium phosphate layer at the dentine-MTA interface when soaked in SBF [57]. It is well recognized that the presence of phosphate ions in the composition of SiO_2-CaO-based materials is not an essential requirement for the formation of apatite spherules. This is because phosphate ions could originate from the physiological solution [56]. The combined effect of Si as an effective apatite nucleator and Ca as an apatite precipitation accelerator leads to apatite precipitation. The in vivo study using rat subcutaneous connective tissues has revealed that the CaSi-based materials produce apatite-like Ca—P crystals at the material–tissue interface [58]. Intriguingly, the apatite-forming ability of the hybrid cement appeared to be related to the type and concentration of the chitosan liquid used. High viscous CTS delayed the precipitation rate of apatite, as verified by the Ca/P ratio. Compared to the stoichiometric Ca/P ratio (1.67) of apatite, the much higher Ca/P ratio of 2.8 for the 1-day-soaked CT1 cement surface was not surprising because a large quantity of calcium originating from the underlying samples was detected. The solubility of chitosan in SBF may also dominate the precipitate rate of apatite. It is speculated that water-insoluble CTS acted as a cohesion/barrier film to reduce calcium release. Contrarily, the Ca/P ratio produced by the water-soluble CS control and CO1 cements was close to the stoichiometric Ca/P ratio of apatite.

Even if bone cement is used in low or non-load-bearing bone defects, it should be paid attention to whether the incorporation of chitosan may jeopardize the mechanical properties of hybrid cement. In fact, the strength value of the hybrid cement prepared from a high concentration of chitosan was higher than that of a low concentration of chitosan. Xu et al. have reported that the addition of chitosan lactate to calcium phosphate cement can increase the flexural strength of cement [59]. The interaction between the organic chitosan and CaSi ceramic matrix can affect the level of reinforcement. When these chitosan biomolecules were added to CaSi, hydrogen bonds and ionic bonds were formed, which increased the diametral tensile strength [60]. The entanglement of viscous chitosan might be another contributive factor [61]. When small organic molecules were uniformly dispersed throughout the ceramic and strongly interacted with the ceramic matrix, the mechanical properties were enhanced. Aforementioned, the added chitosan biomolecules defined the unique properties, such as anti-washout of the hybrid cement. In short, the addition of chitosan had bidirectional and complex effects on characteristics of the CS control cement, which also influenced antibacterial and osteogenic activity.

When soaked in a dynamic SBF solution, the mechanical strength of all cement samples decreased with the increasing time. This is can be explained by the dissolution of CaSi and chitosan, which led to the formation of a porous structure, in concurrence with the porosity results. Water/ions in the solution penetrate into the inner portion of the material through structural defects (such as pores and defects) and come into contact with deeper portions of the material, resulting in weaker structures [62]. Porosity adversely affects the properties of ceramic materials, which may act as a stress raiser to reduce mechanical strength [10]. Not surprisingly, the porosity of all cements increased linearly with soaking time, and the trends were similar. Nevertheless, bone tissue cells could take advantage of the increased porosity to improve the osteogenesis of the implanted material and accelerate its complete transformation into real bone tissue before the samples fractured.

The bioactivity and/or degradation rates of cement samples were also characterized by their weight loss in SBF as a function of soaking time. The current results indicated that the weight loss of all cement systems was relatively small (about 2%) after a 30-day soaking time, after which the weight loss was slightly increased to 4–8%. The formation of apatite, as revealed by SEM observation, may be the main reason for the weight change. Hence, even after extending to 90 days in SBF, there seemed to be no further change. High physiochemical activity and low degradability are the characteristics of the present cement, which are the most important and necessary for the successful results of bone graft substitutes for vertebroplasty [63].

In addition to in vitro bioactivity assays, in vitro cell function examinations also play an important role in the feasibility assessment of biomaterials. Bone cement should support the growth of cells and tissues, thereby enhancing bone regeneration. The behavior of osteoblasts on the surface of the biomaterials depends closely on the physical and chemical properties of the materials. There is concern about whether an antibacterial agent in the cement will damage the osteogenesis of the cells. Thus, the biological function of the hybrid cement was examined by evaluating the in vitro osteogenic activity of MG63 cells cultured on the cement surface. The results of the current study clearly pointed out that compared with the CS control cement, antibacterial agents including CTS, QTS, and COS on the surface of the hybrid cement caused

a certain degree of concentration-dependent cell growth reduction. The expression of cell proliferation, ALP differentiation, and calcium deposits was inversely proportional to the content of biomolecule additives. The membrane-bound exoenzyme ALP is involved in the regeneration of bones at the early stage of osteogenic differentiation, and the ability of cells to produce a mineralized matrix in the material is important for bone regeneration [27]. These results were consistent with the findings of Qi et al., which the inhibitory effect of chitosan nanoparticles on cell viability was clearly observed in a dose-dependent fashion [64]. Peng et al. reported that a higher degree of substitution of quaternary ammonium by reacting chitosan with GTMAC significantly inhibited proliferation and osteogenic differentiation when compared to a lower degree of substitution, although it has a high antibacterial efficiency [65]. On the other hand, the higher degree of deacetylation (DD) of chitosan resulted in higher cell adhesion and viability on the surface [66]. This might explain why the cell viability of COS (DD = 90%) was higher than that of CTS (DD = 85%) at the same concentration.

Advances in bone graft design and surgical techniques are to facilitate the repair and regeneration of bone defect, but the elimination of biomaterial-associated infections is also a crucial factor in the success of a surgical therapy. This is because infections associated with biomaterials can cause great surgical problems that can lead to implant failure. Therefore, the antibacterial materials are placed at the site of infection to inhibit bacterial growth or directly kill bacterial pathogens. In general, the antibacterial efficacy of implant materials is related to the type and concentration of antibacterial agents used [9,33]. It is recognized that the large amount of antibacterial agents added to implant materials induce toxicity, so the used amount must be tailored to pursue high antibacterial and high osteogenic effects. Concerning the antibacterial efficacy of the chitosan used in this study, the current results of the quantitative antimicrobial tests elucidated that all hybrid cements significantly caused a reduction in viable bacteria compared to the CS control, showing type-dependent and concentration-dependent activity.

Two different types of bacteria were used to check the efficacy of antibacterial agents. Gram-negative *E. coli* bacteria is a widespread intestinal parasite of mammals, and Gram-positive *S. aureus* bacteria is one of the major causes of community-acquired and hospital-acquired infections [9]. The growth of *E. coli* and *S. aureus* was clearly observed on the surface of the CS control. It is no doubt that the antibacterial activity of $Ca(OH)_2$ was higher than that of the CS control. Because the strong alkaline pH can effectively eliminate microorganisms, $Ca(OH)_2$ is used as an intracanal medication in endodontic therapy [32]. The lethal effect of OH^- ions on bacterial cells is probably due to the destruction of the bacterial cytoplasmic membrane, structural protein and DNA [67]. Therefore, the alkaline CS control cement containing calcite had bactericidal activity. The CS control cement was not completely effective against *E. coli* and *S. aureus*, it killed only about 30–50% of the bacteria. In view of MG63 cell function, the CS control was higher than other hybrid cements. For example, on the first day of culture, the MG63 cell attachment on the CS control was a 1.9-fold and 1.2-fold higher than that of CT1 and QTS1, respectively, while the bacteriostasis ratio of *E. coli* was about 42% and 51% with respect to CT1 and QT1, respectively. In the case of *S. aureus*, the corresponding bacteriostasis ratio became 32% and 35%. The CS control had higher cell growth than the CT1 and QT1 cements, but 1 wt% CTS and 1 wt% QTS greatly improved the antibacterial activity of the CS control cement.

When chitosan was incorporated with the CaSi cement, it stimulated the bactericidal efficacy to a greater extent than the CS control. Compared with the CS control, the number of rod-shaped *E. coli* and spherical *S. aureus* bacteria adhered on the hybrid cement was appreciably reduced. More importantly, significance to prevent bacterial adhesion was seen in the high concentration of an antibacterial agent on the cement surface. The initial bacterial adhesion depends on the overall physicochemical characteristics of the microbial cell surface, the biomaterial surface, and the biological bathing fluid [9,68]. Hence, it can be speculated that the results of antimicrobial activity was possibly due to a synergic action of the nature (e.g. molecular weight, charge, and degree of deacetylation) of the biomolecules, the pH of the material (and/or environmental), and chitosan-metal complexes [69,70]. Essentially, the interaction between positively-charged chitosan molecules and negatively-charged bacterial membranes results in the leakage of proteinaceous and other intracellular constituents [19]. Rabea et al. pointed out that low concentrations of positively charged chitosan molecules may bind to the surface of negatively charged bacterial, causing bacterial agglutination; at higher concentrations, a larger number of positive charges can make the surface of the bacteria have a net positive charge and keep them suspended [19].

When pH is considered a possible effect, it is conceivable that antibacterial activity of the CTS solution is higher at low environmental pH values, because the amino group of chitosan is ionized at a pH value below 6, thereby increasing the positive charge [69]. Contrarily, when the ambient pH is above pKa (6.3–6.5) of CTS, CTS tends to lose its charge and may precipitate out of solution due to deprotonation of amino groups [70,71]. As evidenced in this study, even with an acid-soluble CTS solution, CTS-containing cements possessed an alkaline pH. High molecular weight and water-insoluble CTS would accumulate on the surface of microbial cells, which in turn form an impermeable layer around the cells because of an alkaline environment [72]. It is expected that this impermeable layer will prevent the transport of essential solutes and may also destroy the cell walls and cause severe leakage of cellular components, ultimately leading to cell death [69,72]. In contrast, the water-soluble chitosan (COS) could not form such a layer so that it had a lower antibacterial efficacy, but there was a lower cytotoxicity than CTS [72]. However, low-molecular-weight COS can permeate into cells and interact with microbial DNA, resulting in suppression of mRNA synthesis and DNA transcription [12,46,69]. According to the literature [73,74], the antibacterial efficacy of chitosan solution against *E. coli* and *S. aureus* increased with its molecular weight. This served to explain why CTS had higher antibacterial activity than COS at the same concentration. Regarding water-soluble QTS at neutral pH, permanent positive charges due to quaternization may be beneficial for the electrostatic interaction [13].

In addition to the above mechanisms, the generation of ROS induced by chitosan might be also one of factors in the antibacterial effectiveness. ROS include superoxide anions, hydroxyl radicals, singlet oxygen, and hydrogen peroxide, which are by-products of cellular oxidative metabolism [33,75]. ROS are important for intracellular signal transduction and destroying pathogens, but excess ROS can destroy lipids, proteins, RNA, and DNA and thus impair cell function [76]. In a study by Raho et al., chitosan-treated tomato cells produced 5 times more ROS than the control without chitosan [77]. Based on current results, the significant increase in ROS depended on the concentration and type of chitosan added. Importantly, the trend of intracellular ROS induced by chitosan was quite coincident with the antibacterial ability, clarifying that higher use concentrations produced higher ROS levels, imparting greater antibacterial activity.

The flexibility of biomolecule introduction may allow for the tunable biological properties and antibacterial efficacy of the bone cements. An appropriate concentration of chitosan could produce remarkably antibacterial efficacy on bacteria without causing large side effects on cell function. The current study clearly showed that the handling properties, antibacterial activity, and osteogenic properties of the hybrid cements can be tailored by using chitosan biomolecule. Despite the osteogenic activity of the CS control was higher than those of all hybrid cements, the introduction of chitosan into the cement obviously improved the antibacterial activity of the CS control. In vitro osteogenesis analysis consistently showed that cells cultured on CO10 and QT1 cement surfaces had significantly higher adhesion, proliferation, ALP expression, and Ca content than those cultured on CT1 cement surfaces, although both cements had lower antibacterial activity.

However, the CO10 cement did not have anti-washout ability, while the CT1 cement had the disadvantage of long setting time. The bacteriostasis ratio of QT1 cement was slightly lower than that of QT5 cement, but its osteogenic activity was significantly higher. Thus, considering the choice between setting time, anti-washout ability, antibacterial effectiveness, and osteogenic activity into account, we could ensure that 1 wt% QTS might be suitable for the liquid phase in the CaSi cement system.

5. Conclusions

In order to impart the bactericidal efficacy of calcium silicate cement, three types of chitosan molecules were used as the liquid phase to mix the calcium silicate powder. To the best of my knowledge, the current study was the first work to systematically explore chitosan/calcium silicate hybrid cements. It can be clearly seen that the CTS and QTS solutions with a concentration of not < 1 wt% may improve the washout resistance of the control cement. Antibacterial assays revealed that the chitosan efficiently inhibited the growth of Gram-positive and Gram-negative bacteria in a dose-dependent fashion, which was also related to the type of chitosan. The results of cell attachment, proliferation, ALP activity, and calcium deposit consistently confirmed a negative correlation between the concentration of chitosan and osteogenic activity in vitro. It is concluded that, when anti-washout properties, setting time, antibacterial activity, and osteogenic activity were taken into account, CaSi cement with 1% QTS may be a good candidate for repairing bone defects. Further investigations, such as in vivo study, are needed to validate the potential bone cements for the clinical applications.

Author statement

Ming-Cheng Lin: Conceptualization, Methodology, Investigation, Visualization, Data Curation, Writing - Original draft preparation.

Chun-Cheng Chen: Data Curation, Validation, Visualization.

I-Ting Wu: Conceptualization, Formal analysis, Writing - Reviewing and Editing.

Shinn-Jyh Ding: Conceptualization, Writing - Reviewing and Editing, Supervision.

Declaration of competing interest

The authors declare that they have no known competing financial interests or personal relationships that could have appeared to influence the work reported in this paper.

References

[1] H.H.K. Xu, S. Takagi, J.B. Quinn, L.C. Chow, Fast-setting calcium phosphate scaffolds with tailored macropore formation rates for bone regeneration, J. Biomed. Mater. Res. A 68 (2004) 725–734.

[2] W.A. Jiranek, A.D. Hanssen, A. Seth Greenwald, Antibiotic-loaded bone cement for infection prophylaxis in total joint replacement, J. Bone Jt. Surg. Am. 88 (2006) 2487–2500.

[3] G. Lewis, Injectable bone cements for use in vertebroplasty and kyphoplasty: state-of-the-art review, J. Biomed. Mater. Res. B 76 (2006) 456–468.

[4] O. Leppäranta, M. Vaahtio, T. Peltola, D. Zhang, L. Hupa, M. Hupa, H. Ylänen, J.I. Salonen, M.K. Viljanen, E. Eerola, Antibacterial effect of bioactive glasses on clinically important anaerobic bacteria in vitro, J. Mater. Sci. Mater. Med. 19 (2008) 547–551.

[5] A. Sugawara, K. Asaoka, S.J. Ding, Calcium phosphate-based cements: clinical needs and recent progress, J. Mater. Chem. B 1 (2013) 1081–1089.

[6] T.Y. Chiang, S.J. Ding, Comparative physicochemical and biocompatible properties of radiopaque dicalcium silicate cement and mineral trioxide aggregate, J. Endod. 36 (2010) 1683–1687.

[7] X. Wang, Y. Zhou, L. Xia, C. Zhao, L. Chen, D. Yi, J. Chang, L. Huang, X. Zheng, H. Zhu, Y. Xie, Y. Xu, K. Lin, Fabrication of nano-structured calcium silicate coatings with enhanced stability, bioactivity and osteogenic and angiogenic activity, Colloids Surf. B: Biointerfaces 126 (2015) 358–366.

[8] A. Ewald, D. Hösel, S. Patel, L.M. Grover, J.E. Barralet, U. Gbureck, Silver-doped calcium phosphate cements with antimicrobial activity, Acta Biomater. 7 (2011) 4064–4070.

[9] C.K. Wei, S.J. Ding, Dual-functional bone implants with antibacterial ability and osteogenic activity, J. Mater. Chem. B 5 (2017) 1943–1953.

[10] C.C. Ho, S.C. Huang, C.K. Wei, S.J. Ding, In vitro degradation and angiogenesis of porous calcium silicate-gelatin composite scaffold, J. Mater. Chem. B 4 (2016) 505–512.

[11] D. Raafat, H.G. Sahl, Chitosan and its antimicrobial potential - a critical literature survey, Microb. Biotechnol. 2 (2009) 186–201.

[12] M. Kong, X.G. Chen, K. Xing, H.J. Park, Antimicrobial properties of chitosan and mode of action: a state of the art review, Int. J. Food Microbiol. 144 (2010) 51–63.

[13] A. Verlee, S. Mincke, C.V. Stevens, Recent developments in antibacterial and antifungal chitosan and its derivatives, Carbohyd. Polym. 164 (2017) 268–283.

[14] T. Wu, X. Hua, Z. He, X. Wang, X. Yu, W. Ren, The bactericidal and biocompatible characteristics of reinforced calcium phosphate cements, Biomed. Mater. 7 (2012) 045003.

[15] A.M. El-Nahrawy, A.I. Ali, A.B. Abou Hammad, A.M. Youssef, Influences of Ag-NPs doping chitosan/calcium silicate nanocomposites for optical and antibacterial activity, Int. J. Biol. Macromol. 93 (2016) 267–275.

[16] A.M. Youssef, A.M. El-Nahrawy, A.B. Abou Hammad, Sol-gel synthesis and characterizations of hybrid chitosan-PEG/calcium silicate nanocomposite modified with ZnO-NPs and (E102) for optical and antibacterial applications, Int. J. Biol. Macromol. 97 (2017) 561–567.

[17] H.K. No, N.Y. Park, S.H. Lee, S.P. Meyers, Antibacterial activity of chitosans and chitosan oligomers with different molecular weights, Int. J. Food Microbiol. 74 (2002) 65–72.

[18] J.K. Francis Suh, H.W.T. Matthew, Application of chitosan-based polysaccharide biomaterials in cartilage tissue engineering: a review, Biomaterials 21 (2000) 2589–2598.

[19] E.I. Rabea, M.E.T. Badawy, C.V. Stevens, G. Smagghe, W. Steurbaut, Chitosan as antimicrobial agent: applications and mode of action, Biomacromolecules 4 (2003) 1457–1465.

[20] S.J. Ding, Biodegradation behavior of chitosan/calcium phosphate composites, J. Non-Crystal. Solids 353 (2007) 2367–2373.

[21] A.M. Youssef, M.S. Abdel-Aziz, S.M. El-Sayed, Chitosan nanocomposite films based on Ag-NP and Au-NP biosynthesis by *Bacillus subtilis* as packaging material, Int. J. Biol. Macromol. 69 (2014) 185–191.

[22] A.M. Youssef, M.E. Abdel-Aziz, E.S.A. El-Sayed, M.S. Abdel-Aziz, A.A. Abd El-Hakim, S. Kamel, G. Turky, Morphological, electrical & antibacterial properties of trilayered Cs/PAA/PPy bionanocomposites hydrogel based on Fe_3O_4-NPs, Carbohyd. Polym. 196 (2018) 483–493.

[23] H.-J. Lee, B. Kim, A.R. Padalhin, B.-T. Lee, Incorporation of chitosan-alginate complex into injectable calcium phosphate cement system as a bone graft material, Mater. Sci. Eng. C 94 (2019) 385–392.

[24] Z. Jia, D. shen, W. Xu, Synthesis and antibacterial activities of quaternary ammonium salt of chitosan, Carbohydr. Res. 333 (2001) 1–6.

[25] N. Vallapa, O. Wiarachai, N. Thongchul, J. Pan, V. Tangpasuthadol, S. Kiatkamjornwong, V.P. Hoven VP, Enhancing antibacterial activity of chitosan surface by heterogeneous quaternization, Carbohyd. Polym. 83 (2011) 868–875.

[26] C.H. Kim, J.W. Choi, H.J. Chun, K.S. Chio, Synthesis of chitosan derivatives with quaternary ammonium salt and their antibacterial activity, Polym. Bull. 38 (1997) 387–393.

[27] I.T. Wu, T.Y. Chiang, C.C. Chen, Y.C. Chen, S.J. Ding, Dopant-dependent tailoring of physicochemical and biological properties of calcium silicate bone cements, Bio-Med. Mater. Eng. 29 (2018) 773–785.

[28] N. Kubota, Y. Eguchi, Facile preparation of water-soluble n-acetylated chitosan and molecular weight dependence of its water-solubility, Polym. J. 29 (1997) 123–127.

[29] R. Tang, Y. Zhang, Y. Zhang, Z. Yu, Synthesis and characterization of chitosan based dye containing quaternary ammonium group, Carbohyd. Polym. 139 (2016) 191–196.

[30] T.Y. Chiang, C.C. Ho, C.H. David Chen, M.H. Lai, S.J. Ding, Physicochemical properties and biocompatibility of chitosan oligosaccharide/gelatin/calcium phosphate hybrid cements, Mater. Chem. Phys. 120 (2010) 282–288.

[31] S.J. Ding, Y.H. Chu, D.Y. Wang, Enhanced properties of novel zirconia-based osteo-implant systems, Appl. Mater. Today 9 (2017) 622–632.

[32] B.C. Wu, C.K. Wei, N.S. Hsueh, S.J. Ding, Comparative cell attachment, cytotoxicity and antibacterial activity of radiopaque dicalcium silicate cement and white-coloured mineral trioxide aggregate, Int. Endod. J. 48 (2015) 268–276.

[33] H. Kao, C.C. Chen, Y.R. Huang, Y.H. Chua, A. Csík, S.J. Ding, Metal ion-dependent tailored antibacterial activity and biological properties of polydopamine-coated titanium implants, Surf. Coat. Technol. 378 (2019) 124998.

[34] A. Gomes, E. Fernandes, J.L.F.C. Lima, Fluorescence probes used for detection of reactive oxygen species, J. Biochem. Biophys. Methods 65 (2005) 45–80.

[35] O.M. Kolawole, W.M. Lau, V.V. Khutoryanskiy, Methacrylated chitosan as a polymer with enhanced mucoadhesive properties for transmucosal drug delivery, Int. J. Pharm. 550 (2018) 123–129.

[36] H. Zheng, Y.M. Du, J.H. Yu, F.H. Huang, L.N. Zhang, Preparation and characterization of chitosan/poly(vinyl alcohol) blend fibers, J. Appl. Polym. Sci. 80 (2001) 2558–2565.

[37] H.Y. Kweon, I.C. Um, Y.H. Park, Structural and thermal characteristics of Antheraea pernyi silk fibroin/chitosan blend film, Polymer 42 (2001) 6651–6656.

[38] H.S. Seong, H.S. Whang, S.W. Ko, Synthesis of a quaternary ammonium derivative of chitooligosaccharide as antimicrobial agent for cellulosic fibers, J. Appl. Polym. Sci. 76 (2000) 2009–2015.

[39] A. Meiszterics, L. Rosta, H. Peterlik, J. Rohonczy, S. Kubuki, P. Henits, K. Sinkó, Structural characterization of gel-derived calcium silicate systems, J. Phys. Chem. A 114 (2010) 10403–10411.

[40] I. García Lodeiro, D.E. Macphee, A. Palomo, A. Fernández-Jiménez, Effect of alkalis on fresh C–S–H gels. FTIR analysis, Cem. Concr. Res. 39 (2009) 147–153.
[41] D.S. Brauer, N. Karpukhina, M.D. O'Donnell, R.V. Law, R.G. Hil, Fluoride-containing bioactive glasses: effect of glass design and structure on degradation, pH and apatite formation in simulated body fluid, Acta Biomater. 6 (2010) 3275–3282.
[42] Z.L. Shi, K.G. Neoh, E.T. Kang, W. Wang, Antibacterial and mechanical properties of bone cement impregnated with chitosan nanoparticles, Biomaterials 27 (2006) 2440–2449.
[43] C.C. Chen, M.H. Lai, W.C. Wang, S.J. Ding, Properties of anti-washout-type calcium silicate bone cements containing gelatin, J. Mater. Sci. Mater. Med. 21 (2010) 1057–1068.
[44] D. Wang, Y. Zhangn, Z. Hong, Novel fast-setting chitosan/β-dicalcium silicate bone cements with high compressive strength and bioactivity, Ceram. Int. 40 ((2014) 9799–9808.
[45] H. Zhang, S.H. Neau, In vitro degradation of chitosan by a commercial enzyme preparation: effect of molecular weight and degree of deacetylation, Biomaterials 22 (2001) 1653–1658.
[46] P. Zou, X. Yang, J. Wang, Y. Li, H. Yu, Y. Zhang, G. Liu, Advances in characterisation and biological activities of chitosan and chitosan oligosaccharides, Food Chem. 190 (2016) 1174–1181.
[47] K. Ishikawa, Y. Miyamoto, M. Takechi, T. Toh, M. Kon, M. Nagayama, K. Asaoka, Non-decay type fast-setting calcium phosphate cement: hydroxyapatite putty containing an increased amount of sodium alginate, J. Biomed. Mater. Res. 36 (1997) 393–399.
[48] K. Tappa, U. Jammalamadaka, D.K. Mills, Formulation and evaluation of nanoenhanced anti-bacterial calcium phosphate bone cements, in: B. Li, T. Webster (Eds.), Orthopedic Biomaterials, Springer, Switzerland, 2007, pp. 85–108.
[49] M. Takechi, Y. Miyamoto, K. Ishikawa, M. Yuasa, M. Nagayama, M. Kon, K. Asaoka, Non-decay type fast-setting calcium phosphate cement using chitosan, J. Mater. Sci. Mater. Med. 7 (1996) 317–322.
[50] X. Wang, L. Chen, H. Xiang, J. Ye, Influence of anti-washout agents on the rheological properties and injectability of a calcium phosphate cement, J. Biomed. Mater. Res. B 81 (2007) 410–418.
[51] M.A.H. Duarte, K. Alves de Aguiar, M.A. Zeferino, R.R. Vivan, R. Ordinola-Zapata, M. Tanomaru-Filho, P.H. Weckwerth, M.C. Kuga, Evaluation of the propylene glycol association on some physical and chemical properties of mineral trioxide aggregate, Int. Endod. J. 45 (2012) 565–570.
[52] M.Y. Shie, H.C. Chang, S.J. Ding, Composition-dependent protein secretion and integrin level of osteoblastic cell on calcium silicate cements, J. Biomed. Mater. Res. A 102 (2014) 769–780.
[53] Q. Lin, X. Lan, Y. Li, Y. Yu, Y. Ni, C. Lu, Z. Xu, Anti-washout carboxymethyl chitosan modified tricalcium silicate bone cement: preparation, mechanical properties and in vitro bioactivity, J. Mater. Sci. Mater. Med. 21 (2010) 3065–3076.
[54] F. Panahi, S.M. Rabiee, R. Shidpour, Synergic effect of chitosan and dicalcium phosphate on tricalcium silicate-based nanocomposite for root-end dental application, Mater. Sci. Eng. C 80 (2017) 631–641.
[55] S.J. Ding, Preparation and properties of chitosan/calcium phosphate composites for bone repair, Dent. Mater. J. 25 (2006) 706–712.
[56] C.C. Chen, C.W. Wang, N.S. Hsueh, S.J. Ding, Improvement of in vitro physicochemical properties and osteogenic activity of calcium sulfate cement for bone repair by dicalcium silicate, J. Alloys Compd. 585 (2014) 25–31.
[57] J.R. Kim, A. Nosrat, A.F. Fouad, Interfacial characteristics of biodentine and MTA with dentine in simulated body fluid, J. Dent. 43 (2015) 241–247.
[58] G. Hinata, K. Yoshiba, L. Han, N. Edanami, N. Yoshiba, T. Okiji, Bioactivity and biomineralization ability of calcium silicate-based pulp-capping materials after subcutaneous implantation, Int. Endod. J. 50 (2017) e40–e51.
[59] H.H.K. Xu, J.B. Quinn, S. Takagi, L.C. Chow, Processing and properties of strong and non-rigid calcium phosphate cement, J. Dent. Res. 81 (2002) 219–224.
[60] D.X. Li, H.S. Fan, X.D. Zhu, Y.F. Tan, W.Q. Xiao, J. Lu, Y.M. Xiao, J.Y. Chen, X.D. Zhang, Controllable release of salmon-calcitonin in injectable calcium phosphate cement modified by chitosan oligosaccharide and collagen polypeptide, J. Mater. Sci. Mater. Med. 18 (2007) 2225–2231.
[61] R.H. Chen, H.-D. Hwa, Effect of molecular weight of chitosan with the same degree of deacetylation on the thermal, mechanical, and permeability properties of the prepared membrane, Carbohyd. Polym. 29 (1996) 353–358.
[62] C.C. Chen, W.C. Wang, S.J. Ding, In vitro physiochemical properties of gelatin/chitosan oligosaccharide/calcium silicate hybrid cement, J. Biomed. Mater. Res B 59 (2010) 456–465.
[63] P.F. Heini, U. Berlemann, Bone substitutes in vertebroplasty, Eur. Spine J. 10 (2001) S205–S213.
[64] L.F. Qi, Z.R. Xu, Y. Li, X. Jiang, X.Y. Han, In vitro effects of chitosan nanoparticles on proliferation of human gastric carcinoma cell line MGC803 cells, World J. Gastroenterol. 11 (2005) 5136–5141.
[65] Z.-X. Peng, L. Wang, L. Du, S.-R. Guo, X.-Q. Wang, T.-T. Tang, Adjustment of the antibacterial activity and biocompatibility of hydroxypropyltrimethyl ammonium chloride chitosan by varying the degree of substitution of quaternary ammonium, Carbohyd. Polym. 81 (2010) 275–283.
[66] C. Chatelet, O. Damour, A. Domard, Influence of the degree of acetylation on some biological properties of chitosan films, Biomaterials 22 (2001) 261–268.
[67] J.F. Siqueira Jr., H.P. Lopes, Mechanisms of antimicrobial activity of calcium hydroxide: a critical review, Int. Endod. J. 32 (1999) 361–369.
[68] H. Van de Belt, D. Neut, W. Schenk, J.M. Van Horn, H.C. Van der Mei, H.J. Busscher, Acta Orthop. Scand. 72 (2001) 557–571.
[69] M. Hosseinnejad, S.M. Jafari, Evaluation of different factors affecting antimicrobial properties of chitosan, Int. J. Biol. Macromol. 85 (2016) 467–475.
[70] X. Wang, Y. Du, L. Fan, H. Liu, Y. Hu, Chitosan-metal complexes as antimicrobial agent: synthesis, characterization and structure-activity study, Polym. Bull. 55 (2005) 105–113.
[71] E. Guibal, Interactions of metal ions with chitosan-based sorbents: a review, Sep. Purif. Technol. 38 (2004) 43–74.
[72] C. Qin, H. Li, Q. Xiao, Y. Liu, J. Zhu, Y. Du, Water-solubility of chitosan and its antimicrobial activity, Carbohyd. Polym. 63 (2006) 367–374.
[73] Y.J. Jeon, P.J. Park, S.K. Kim, Antimicrobial effect ofchitooligosaccharides produced by bioreactor, Carbohyd. Polym. 44 (2001) 71–76.
[74] K. Azuma, S. Ifuku, T. Osaki, Y. Okamoto, S. Minami, Preparation and biomedical applications of chitin and chitosan nanofibers, J. Biomed. Nanotechnol. 10 (2014) 2891–2920.
[75] P.P. Fu, Q. Xia, H.M. Hwang, P.C. Ray, H. Yu, Mechanisms of nanotoxicity: generation of reactive oxygen species, J. Food Drug Anal. 22 (2014) 64–75.
[76] K. Ito, T. Suda, Metabolic requirements for the maintenance of self-renewing stem cells, Nature Rev. Mol. Cell Biol. 15 (2014) 243–256.
[77] N. Raho, L. Ramirez, M.L. Lanteri, G. Gonorazky, L. Lamattina, A. ten Have, A.M. Laxalt, Phosphatidic acid production in chitosan-elicited tomato cells, via both phospholipase D and phospholipase C/diacylglycerol kinase, requires nitric oxide, J. Plant Physiol. 168 (2011) 534–539.